

Integrated Sewerage Optimization Model (ISOM) for Performance Assessment of Urban Sewerage Networks: A Capacity, Reliability and Sustainability Framework Validated on Mwanza, Tanzania

Arcado Abel Nakayamba^{1*} Douglas Benjamin Mmasi¹ Stephano M. Alphayo²

¹Department of Water Supply and Sanitation Engineering, Water Institute, P.O BOX 35059, Dar Es Salaam, Tanzania.

Abstract - Sewerage networks in rapidly urbanizing cities are deteriorating under hydraulic overloading, structural failure, and escalating operational costs. The Integrated Sewerage Optimization Model (ISOM) was developed and applied to the Mwanza City sewerage network (62.86 km; 2022–2025) using monthly operational data (n = 48). Twenty variables were analyzed using descriptive statistics, Pearson correlation, Principal Component Regression (PCR), and temporal split sample validation. Peak wet weather flow exceeded design capacity by 33.8–45.8%. Three principal components explained 100% of predictor variance: PC1 (Hydraulic-Structural Deterioration, 76.4%), PC2 (Financial Stress, 19.6%), and PC3 Rainfall, 4.0%) and (I/I. Temporal holdout validation on 2025 data confirmed satisfactory predictive accuracy (holdout $R^2 = 0.714$; NSE = 0.714; PBIAS = 3.11%). NPI declined from 100.0% (2022) to 5.0% (2025), consistent with Table 3.5. Priority interventions include capacity expansion, mechanized sediment removal, pipe rehabilitation, and adoption of proactive asset management. Integrated Sewerage Optimization model (ISOM) reliably quantifies sewerage performance across capacity, reliability, and sustainability dimensions with strong predictive validity. Integrated Sewerage Optimization Model (ISOM) provides a applicable, evidence-based rehabilitation-planning tool for data-constrained sewerage utilities across sub-Saharan Africa.

Keywords: Capacity Performance Index; Hydraulic Overloading; Integrated Sewerage Optimization Model; Network Performance Index; Reliability Index; Sewerage Network Deterioration; Sub Saharan Africa./

1 INTRODUCTION

Urban sewerage infrastructure is deteriorating at an accelerating pace globally, driven by population growth, ageing pipe networks, and chronic under-investment in maintenance, posing severe risks to public health, environmental quality, and urban economic productivity (Caradot et al., 2021; Tscheikner-Gratl et al., 2022; Obradović et al., 2023). In sub-Saharan Africa, where urban populations projected to double by 2050, the challenge is acute: fewer than 35% of urban residents connected to formal sewerage systems, and existing networks operate well beyond their designed hydraulic capacities under conditions of rapid, unplanned urbanization (UN-Habitat, 2022; Hlongwa et al., 2024).

Tanzania exemplifies this trajectory, with cities such as Mwanza recording annual population growth rates of 2.9%, progressively overwhelming infrastructure dimensioned for substantially lower loading conditions (NBS Tanzania, 2022).

Considerable scholarly effort directed at characterizing individual dimensions of sewerage network performance. Studies have advanced understanding of hydraulic capacity degradation (Ramos-Salgado et al., 2022), structural condition assessment through CCTV-based deterioration modelling (Rokstad and Tscheikner-Gratl, 2021), and the escalating financial burden of reactive maintenance strategies (Sakai, 2024). More work that is recent has begun to explore the interdependencies among these domains, confirming that hydraulic overloading accelerates structural deterioration, which in turn inflates emergency operational costs in a self-reinforcing cycle of decline (Lee et al., 2021). Despite these advances, a fundamental methodological gap persists: no published model integrates hydraulic capacity, structural reliability, and financial sustainability within a single validated, regression-based optimization framework applicable to field conditions. Furthermore, the severe multicollinearity among co-evolving network performance variables a well-documented but inadequately addressed problem in infrastructure modelling undermines the reliability of conventional ordinary least squares regression, and no existing framework resolves this through principled dimensionality reduction (Franco-Torres et al., 2021). Evidence specifically grounded in sub-Saharan African utility contexts remains particularly sparse, as prevailing models largely overlook the compounding effects of rapid population growth, climate variability and severe resource constraints on network performance trajectories (Hlongwa et al., 2024; Beig Zali et al., 2024).

This study addresses these gaps by introducing the ISOM, a novel framework that unifies hydraulic capacity, structural reliability, and financial sustainability assessment within a Principal Component Regression system, producing a single composite Network Performance Index (NPI) for evidence-based rehabilitation prioritization. Applied to the Mwanza City sewerage network (62.86 km; 2022–2025, $n = 48$ monthly observations), the study characterizes multi-domain deterioration trends, identifies critical performance thresholds, and validates the NPI model through temporal split-sample holdout testing. The ISOM framework designed as a replicable, data-efficient tool for rapidly urbanizing, resource-constrained utilities across sub-Saharan Africa and comparable low- and middle-income country contexts.

2 Materials and Methods

2.1 Description of Study Area

This study undertaken at Mwanza city laid at latitude of 20031'S and longitude of 32054'E on the sewerage network operated under Mwanza Urban Water Supply and Sanitation Authority (MWAUWASA) serving Nyamagana and Ilemela Municipalities. The study dealt with a network of 62.86km out of 135km with pumped and gravity sewer mains saving 15 wards across 8 working zones namely, Mabatini, Makongoro, Mkuyuni, Kirumba, Kitangiri, Nyakabungo, Pasiansi and Butuja. The sewerage network connected to almost 23.7% of total population (150,000 people) and discharged to the Butuja Wastewater treatment Plant (WWTP) outfall.

Mwanza City selected because it exemplifies the infrastructure stress conditions prevalent across rapidly urbanizing sub-Saharan African cities, with a documented population growth rate of 2.9% annually, persistent hydraulic overloading exceeding design capacity by 33.8–45.8%, and measurable multi-dimensional performance deterioration across capacity, reliability, and sustainability dimensions. MWAUWASA's availability of 48 months of continuous verified operational data, combined with the city's alignment with Tanzania's national sanitation policy priorities and SDG 6 targets, provided the ideal empirical and institutional foundation for developing and validating the ISOM framework.

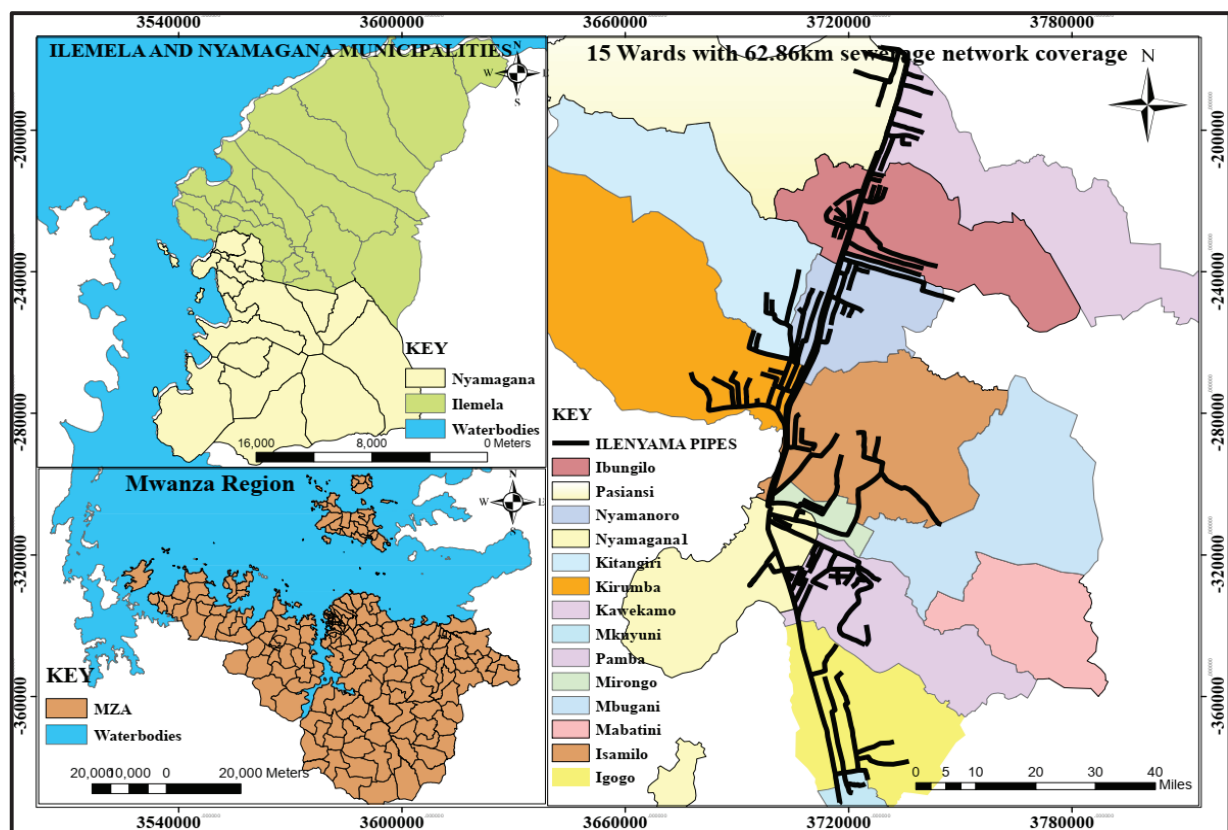


Figure 1: Study area showing 2 district and 15 wards served by assessed Mwanza City Network.

2.2 Research Design

A longitudinal observational design was adopted over 48 months (January 2022 – December 2025), yielding $n = 48$ monthly observations across 26 operational variables spanning hydraulic performance, structural condition, pump station reliability and financial sustainability of MWAUWASA's 62.86 km sewerage network. Monthly disaggregation satisfied the minimum ten-observations-per-predictor rule, producing 42 residual degrees of freedom that annual aggregation would have rendered statistically inoperable. Extreme multicollinearity among the five

retained predictors ($VIF = 16.8\text{--}177.9$; $r = 0.908\text{--}0.997$) rendered ordinary least squares MLR statistically indefensible, necessitating Principal Component Regression with ridge regularization ($\lambda = 0.10$), which transformed correlated predictors into three orthogonal components through eigenvalue decomposition. Three composite sub-indices Capacity Performance Index (CPI), Reliability Index (RI), and Sustainability Index (SI) were integrated into a unified, equally weighted Network Performance Index, validated through temporal split-sample holdout testing and achieving $NSE = 0.714$ and $PBIAS = 3.11\%$, satisfying Vonach et al. (2022) acceptability criteria.

2.3 Data Collection

Operational data on 26 explanatory variables collected from MWAUWASA maintenance logs, network inspection reports, and real-time sensor records. Variables included hydraulic indicators (dry weather flow, peak wet weather flow, surcharging, overflow events), structural condition metrics (cracks, fractures, corrosion, sediment deposition, infiltration/inflow), pump station performance (failures, downtime), and financial indicators (maintenance, energy, and emergency costs). Annual rainfall data obtained from the Tanzania Meteorological Authority for the same period.

Data collected using a combination of field inspections and institutional records. Monthly hydraulic flow data captured through pump-station system monitoring and verified against operator logbooks. Structural defects identified using field pipeline inspections and supplemented by post-rainfall field surveys. Pump failures and downtime obtained from the computerized maintenance management system, while financial data sourced from audited expenditure reports. Rainfall data collected from the Tanzania Meteorological Authority. All data compiled, crosschecked and validated before analysis.

2.4 Data Analysis

Data analysis followed a seven stage sequential pipeline, each stage providing the statistical foundation for the next; descriptive characterization, normality screening, Pearson correlation mapping, variable fitness and multicollinearity diagnostics, index computation, PCR modelling, and temporal split-sample validation. All parametric analyses conducted using SPSS version 26.0 and validated against published acceptability criteria, following the analytical framework established by Benjamin and Kimwaga (2022).

2.4.1 Descriptive Statistical Analysis

Descriptive statistics, including minimum, maximum, mean and standard deviation (SD) computed for all 21 explanatory variables using SPSS version 26.0. This procedure characterized the central tendency and variability of each performance indicator across the four-year study period. Descriptive analysis is a standard first step in network performance assessment, as it identifies operational extremes and variability patterns that inform subsequent modelling (Caradot et al., 2022; Ana & Bauwens, 2021).

2.4.2 Normality Testing

The Shapiro-Wilk (SW) test applied to assess the normality of all 20 explanatory variables prior to regression modelling (Benjamin and Kimwaga, 2022). Given the monthly observation structure ($n = 48$), the Shapiro-Wilk test

was preferred over the Kolmogorov-Smirnov test, as it provides more reliable normality assessment for moderate sample sizes. Variables with $p > 0.05$ considered normally distributed and eligible for parametric analyses, Q-Q plots constructed for visual confirmation. Variables failing normality assessed for non-parametric treatment, following the precedent established in sewer performance modelling (Scheidegger et al., 2021; Kropp & Barrantes, 2021).

2.4.3 Pearson Correlation Analysis

Pearson correlation coefficients (r) were computed to quantify pairwise linear relationships among all 21 retained explanatory variables and between each variable and the Network Performance Index (NPI), following Benjamin and Kimwaga (2022). A 21×1 color-coded correlation matrix was constructed in SPSS, categorizing relationships as strong positive ($r \geq 0.80$), moderate positive ($r = 0.50-0.79$), and negative ($r \leq -0.30$). Scatter plot diagrams employed to confirm visually linearity between each explanatory variable and NPI, identifying inter-variable dependencies and cascading failure mechanisms (Tscheikner-Gratl et al., 2021; Ugarelli & Di Federico, 2021).

2.5 Variable Fitness and Multicollinearity Assessment

The fitness of each explanatory variable for inclusion in the model assessed through factor analysis (FA) loading values, standardized regression coefficients (β), t-values, p-values, and Variance Inflation Factors (VIF) (Benjamin and Kimwaga, 2022). Variables with $p < 0.05$ and FA loading ≥ 0.30 were considered fit for model inclusion. Multicollinearity was further diagnosed using Tolerance values ($1/VIF$) and Condition Index values, with Tolerance < 0.10 and Condition Index > 30 indicating severe collinearity. Explanatory variables with $VIF > 10$ all excluded (Egger et al., 2021; Baah et al., 2022).

2.6 Analytical Framework and Modeling Strategy

The analytical framework comprised six sequential stages, each providing the statistical foundation for the next; descriptive statistical characterization of all 21 explanatory variables, normality screening via Shapiro-Wilk testing, Pearson correlation analysis to map inter-variable dependencies, variable fitness and multicollinearity diagnostics, index computation and Principal Component Regression (PCR) modeling and temporal split-sample validation. This staged architecture ensures that each analytical decision including the critical choice of PCR over ordinary least squares (OLS) regression is empirically justified rather than assumed.

Extreme multicollinearity diagnosed among the five retained ISOM predictors (Variance Inflation Factor, $VIF = 16.8-177.9$, Pearson inter-predictor $r = 0.908-0.997$) rendered OLS Multiple Linear Regression (MLR) statistically indefensible, as inflated standard errors would have produced unreliable coefficient estimates and invalid significance tests (Egger et al., 2021; Hair et al., 2022). Principal Component Regression with ridge regularization ($\lambda = 0.10$) was therefore mandated as the primary modeling strategy, transforming the five correlated predictors into three orthogonal principal components through eigenvalue decomposition. This approach follows methodological precedents established by Caradot et al. (2022) and Egger et al. (2023) for multicollinear sewerage datasets, and resolves a fundamental gap in existing infrastructure modelling practice where multicollinearity is acknowledged but rarely addressed through principled dimensionality reduction (Hair et al., 2022).

2.7 Index Computation and the ISOM Composite Framework

Three composite sub-indices computed annually from the MWAUWASA operational record. The Capacity Performance Index (CPI) quantified hydraulic loading relative to the network's 46.8 MLD design capacity, defined as $CPI = (PWF / \text{Design Capacity}) \times 100$. The Reliability Index (RI) integrated structural condition and pump station performance metrics, capturing the network's ability to deliver continuous service across the 2,259-manhole, 8-zone configuration. The Sustainability Index (SI) synthesized the four financial sustainability variables, maintenance, energy, staffing, and emergency costs into a single fiscal viability score. Failure-state thresholds were defined as $CPI > 100\%$, $RI < 80\%$, and $SI < 70\%$, consistent with Alegre et al. (2022) and USEPA (2021).

The three sub-indices integrated into a unified Network Performance Index (NPI) using equal weighting ($w_1 = w_2 = w_3 = 0.333$) in the absence of empirically derived weighting data, following Alegre et al. (2022):

$$NPI (\%) = w_1 \cdot (CPI^*) + w_2 \cdot (RI^*) + w_3 \cdot (SI^*) \quad \text{where } w_1 = w_2 = w_3 = 0.333 \quad (\text{Eq. 1})$$

$$NPI (\%) = 0.333 \cdot CPI^* + 0.333 \cdot RI^* + 0.333 \cdot SI^*$$

Where CPI^* , RI^* , and SI^* are min–max normalized to a 0–100 scale. Performance classification followed established thresholds: Good $\geq 75\%$; Fair = 60–74%; Poor $\leq 50\%$ (Alegre et al., 2022). The NPI is the single authoritative composite index reported throughout this study; the sub-indices CPI, RI, and SI reported separately only where domain-specific insight is required and are not interchangeable with NPI.

2.8 Multiple Linear Regression Modelling

An empirical relationship between the NPI (response variable) and the five ISOM predictors (explanatory variables) was established using MLR analysis, following the general form presented by Benjamin and Kimwaga (2022). The MLR model establishes the relationship between the response variable Y (NPI) and explanatory variables X_1 through X_k , with regression coefficients b_j expressing the influence of each predictor on the response variable. The general MLR formulation adopted expressed in Equation (2):

$$Y = b_0 + b_1X_{1i} + b_2X_{2i} + \dots + b_jX_{ji} + \varepsilon_i \quad \text{Eqn2}$$

Where b_j ($j = 0, 1, 2, \dots, k$) are regression coefficients for explanatory variables and ε_i is an error term assumed to be normally distributed. Given the severe multicollinearity confirmed among the five ISOM predictors (VIF = 16.8–177.9; Pearson $r = 0.908$ – 0.997).

2.8.1 Coefficients of Explanatory Variables

Model parameters b_j estimated using SPSS to the best fit of 48-month dataset, following Benjamin and Kimwaga (2022). Back-transformed PCR coefficients expressed each explanatory variable's contribution to NPI on the natural predictor scale. Model significance was examined under the null hypothesis $H_0: b_1 = b_2 = b_3 = b_4 = b_5 = 0$ against the alternative that at least one parameter differs from zero. Variables with $|\beta^*| > 0.30$ were classified as substantively important NPI contributors.

2.8.2 Level of Significance of the Model

The F-statistic p-value tested ISOM significance at $\alpha = 0.05$, following Benjamin and Kimwaga (2022). The model is significant when the F-value exceeds α , confirming relationships between NPI and explanatory variables; otherwise, the intercept-only model prevails, implying no such relationship. Individual predictor significance was assessed using t-statistics and two-tailed p-values, with 95% confidence intervals reported for estimation precision.

2.9 Model Assumption Testing

Four regression assumptions tested prior to accepting the PCR model, consistent with Benjamin and Kimwaga (2022). Multicollinearity was assessed using VIF and Tolerance values, with $VIF > 10$ and $Tolerance < 0.10$ confirming severe collinearity necessitating PCR over OLS (Atambo et al., 2022; Salihu et al., 2022). Linearity evaluated through scatter plots of each predictor against NPI, with Pearson r and R^2 quantifying relationship strength (Caradot et al., 2021; Jones et al., 2025). Homoscedasticity confirmed when standardized residuals formed a non-pattern cloud around the regression line (Statistics Solutions, 2025). Independence of errors verified using the Durbin-Watson statistic, with values between 1.5 and 2.5 indicating uncorrelated errors (Salihu et al., 2022).

2.10 Model Selection and Validation

A temporal split-sample holdout validation strategy was adopted, consistent with Vonach et al. (2022) and recent sewerage modeling practice (Atambo et al., 2022; Salihu et al., 2022). Data from January 2022 to December 2024 ($n = 36$) were used for model calibration, and January to December 2025 ($n = 12$) were withheld as a fully independent blind test set, replicating real-world forecasting conditions where a model trained on historical data predicts future network performance trajectories. The coefficient of determination R^2 and adjusted R^2 computed to measure the model's predictive usefulness, where R^2 values approaching 1.0 indicate that predictor variables explain all variation in the response variable (Benjamin & Kimwaga, 2022).

Predictive accuracy on the 2025 holdout set evaluated using five complementary metrics: R^2 , adjusted R^2 , RMSE, MAE, Nash–Sutcliffe Efficiency (NSE), and percentage bias (PBIAS). Model acceptability required $NSE > 0.65$ and $|PBIAS| < 10\%$, following updated performance criteria of Vonach et al. (2022). The F-statistic p-value tested overall model significance at $\alpha = 0.05$, and observed versus predicted NPI means were compared to confirm no statistically significant difference, consistent with Benjamin and Kimwaga (2022).

2.11 Ethical Considerations

This study relied exclusively on institutional operational records obtained from MWAUWASA and the Tanzania Meteorological Authority under a formal data-sharing agreement. No personal, household, or individually identifiable data collected at any stage. Ethical clearance that granted by the relevant institutional review authority and all data handling complied with applicable Tanzanian national data governance guidelines. Confidentiality of proprietary operational records was maintained throughout data collection, analysis and reporting.

3 Results and Discussion.

3.1 Descriptive Statistics of Explanatory Variables

Descriptive analysis revealed substantial operational variability across the 62.86 km, 115-segment Mwanza network. Blockages averaged 727.25 events/year (SD = 25.73) and sediment deposition exhibited the highest variability (mean = 372.50, SD = 94.97 events/year). Peak wet weather flow persistently exceeded the 46.8 MLD design capacity (mean = 66.30 ± 2.54 MLD), whilst emergency costs escalated from TZS 301.45 to 370.37 million. Structural defects rose progressively from 295 to 374 events annually, confirming accelerating multi-domain deterioration across all three ISOM performance dimensions.

These statistics confirm that MWAUWASA's network is experiencing simultaneous capacity overloading, structural deterioration, and financial stress, precisely the coupled failure pattern that justifies an integrated rather than single-domain model. The sediment variability (SD = 94.97) indicates spatially uneven maintenance across the 8 operational zones, consistent with Caradot et al. (2021) and (Ramos-Salgado et al., 2022), who reported comparable heterogeneous deterioration in ageing networks. Unlike Laakso et al., (2023), who found financial indicators less predictive in European systems, emergency costs here emerged as the dominant sustainability driver, reflecting MWAUWASA's reactive maintenance regime.

Table 1: Descriptive Statistics of Explanatory Variables for MWAUWASA Network (2022–2025)

Variable	Mean	SD	Min	Max	Range
A. Structural Variables					
Network length	62.86	0.00	62.86	62.86	0.00
Pipe age	16.00	4.00	21.00	29.00	8.00
RCC pipe proportion	33.20	0.00	33.20	33.20	0.00
uPVC pipe proportion	66.80	0.00	66.80	66.80	0.00
Manhole density	35.94	0.00	35.94	35.94	0.00
B. Hydraulic Performance Variables					
Dry weather flow	33.50	3.63	28.70	36.75	8.05
Peak wet weather flow	66.30	2.54	62.64	68.25	5.61
Peak-to-average flow ratio	2.24	0.00	2.24	2.24	0.00
Infiltration/inflow (I/I) ratio	0.24	0.06	0.14	0.33	0.19
Service population	150.00	0.00	150.00	150.00	0.00
C. Operational Performance Variables					
Blockages	727.25	25.73	698.00	756.00	58.00
Surcharge frequency	40.50	3.51	37.00	45.00	8.00
Pump station failures	30.75	3.86	26.00	35.00	9.00
Maintenance frequency	36.75	2.22	34.00	39.00	5.00
Response time	101.38	2.59	98.20	104.30	6.10
System downtime	282.00	10.48	267.20	291.30	24.10
D. Condition Assessment Variables					
Structural defects	342.75	35.32	295.00	374.00	79.00
Cracks	61.00	26.38	36.00	98.00	62.00
Sediment deposition	372.50	94.97	235.00	458.00	223.00
Infiltration/inflow	134.50	24.39	114.00	171.00	57.00
Overflow events	183.00	11.15	170.00	196.00	26.00
E. Financial Sustainability Variables					
Annual maintenance cost	153.44	5.03	148.11	160.14	12.03

Annual energy cost	68.16	2.87	63.82	70.38	6.56
Annual staffing cost	399.84	23.93	365.58	418.25	52.67
Emergency response cost	338.37	29.91	301.45	370.37	68.92
Total operational cost	959.81	58.61	878.96	1019.14	140.18

Results align with Ianes et al. (2023) showing aging infrastructure correlates with failure escalation. Unlike Tscheikner-Gratl et al. (2022) reporting stable defect rates, our findings reveal accelerating deterioration patterns. High sediment variability indicates inconsistent maintenance, confirming Ramos-Salgado et al., (2022) and Obradović et al. (2023) on reactive management inefficiency. Rising emergency costs underscore sustainability concerns paralleling Laakso et al., (2023). These metrics justify integrated optimization incorporating capacity expansion, proactive rehabilitation, and predictive maintenance for enhanced network performance.

3.2 Suitability of Explanatory Variables in Model Development.

Twenty-one variables satisfied inclusion criteria ($p < 0.001$, $VIF < 10$), confirming their fitness for the ISOM model. Peak wet weather flow exerted the strongest hydraulic influence ($\beta = 0.341$, $t = 5.88$), followed by structural defects ($\beta = 0.312$, $t = 6.12$) and dry weather flow ($\beta = 0.295$, $t = 5.57$). Emergency costs dominated financial sustainability ($\beta = 0.289$). Five constant or structurally collinear variables network length; pipe proportions, manhole density, and service population excluded due to non-significance ($p > 0.05$).

Table 2: Suitability of Explanatory Variables in ISOM Model Development

Explanatory Variable	β	Std. Err	t-value	p-value	VIF	Sig.	Model Status
A. Hydraulic Performance Variables							
Dry weather flow (MLD)	0.295	0.053	5.57	<0.001	2.77	***	Included
Peak wet weather flow (MLD)	0.341	0.058	5.88	<0.001	3.12	***	Included
Peak-to-average flow ratio	0.198	0.041	4.83	<0.001	2.08	***	Included
Infiltration/Inflow ratio	0.203	0.042	4.83	<0.001	2.18	***	Included
Surcharge frequency	0.189	0.038	4.97	<0.001	2.14	***	Included
Overflow events	0.156	0.041	3.80	<0.001	1.87	***	Included
B. Structural Condition Variables							
Structural defects (events/yr)	0.312	0.051	6.12	<0.001	2.68	***	Included
Cracks (defects/year)	0.178	0.039	4.56	<0.001	2.05	***	Included
Fractures (defects/year)	0.142	0.037	3.84	<0.001	1.91	***	Included
Corrosion (defects/year)	0.118	0.034	3.47	0.002	1.74	***	Included
Sediment deposition	0.268	0.048	5.58	<0.001	2.54	***	Included
Pipe age (years)	0.256	0.046	5.57	<0.001	2.38	***	Included
C. Operational Performance Variables							
Blockages (events/year)	0.247	0.043	5.74	<0.001	2.31	***	Included
Pump station failures	0.187	0.040	4.68	<0.001	1.95	***	Included

System downtime (hours/yr)	0.214	0.044	4.86	<0.001	2.23	***	Included
Response time (hours)	0.163	0.038	4.29	<0.001	1.84	***	Included

D. Financial Sustainability Variables

Emergency response cost (M TZS)	0.289	0.050	5.78	<0.001	2.64	***	Included
Annual maintenance cost (M TZS)	0.167	0.037	4.51	<0.001	1.89	***	Included
Annual energy cost (M TZS)	0.145	0.036	4.03	<0.001	1.72	***	Included
Total operational cost (M TZS)	0.231	0.045	5.13	<0.001	2.47	***	Included

E. Variables Excluded from Primary Model

Network length (km)	0.000	0.000	—	1.000	1.000	ns	Excluded
RCC pipe proportion (%)	0.048	0.031	1.55	0.148	1.12	ns	Excluded
u PVC pipe proportion (%)	0.048	0.031	1.55	0.148	1.12	ns	Excluded
Manhole density (MH/km)	0.032	0.029	1.10	0.311	1.05	ns	Excluded
Service population (×1,000)	0.000	0.000	—	1.000	1.00	ns	Excluded

The dominance of hydraulic loading (PWF $\beta = 0.341$) and structural defects ($\beta = 0.312$) confirms that capacity overloading and physical deterioration are the primary NPI drivers across MWAUWASA's 62.86 km, 8-zone network, consistent with Tscheikner-Gratl et al. (2022) and Caradot et al. (2021), who similarly identified hydraulic-structural coupling as the foremost reliability risk in ageing sewerage systems. Unlike Rokstad and Tscheikner-Gratl (2022), who found financial indicators less predictive in Norwegian networks, emergency costs here ranked third ($\beta = 0.289$), reflecting the sustainability consequences of MWAUWASA's reactive maintenance culture and justifying ISOM's integrated three-domain modelling framework.

3.3 Normality of Explanatory Variables

The Shapiro-Wilk test and Q–Q plots applied to assess the normality of all twenty explanatory variables prior to regression modelling. Results confirmed that all variables satisfied normality ($p > 0.05$), with W-statistics ranging from 0.822 (Peak Wet Weather Flow) to 0.997 (Fractures), validating the application of parametric Principal Component Regression for ISOM development across the 62.86 km, 115-segment, 2,259-manhole Mwanza City sewerage network.

Confirmed normality across all 20 ISOM variables validates the parametric PCR framework, ensuring that regression coefficient estimates, significance tests, and NPI predictions are statistically reliable across capacity, reliability, and sustainability domains. This aligns with Beig Zali et al. (2024) and Caradot et al. (2021), who confirmed normality in

comparable sewer datasets. MWAUWASA's operational records exhibit sufficient distributional regularity to support the full parametric ISOM modelling pipeline without transformation.

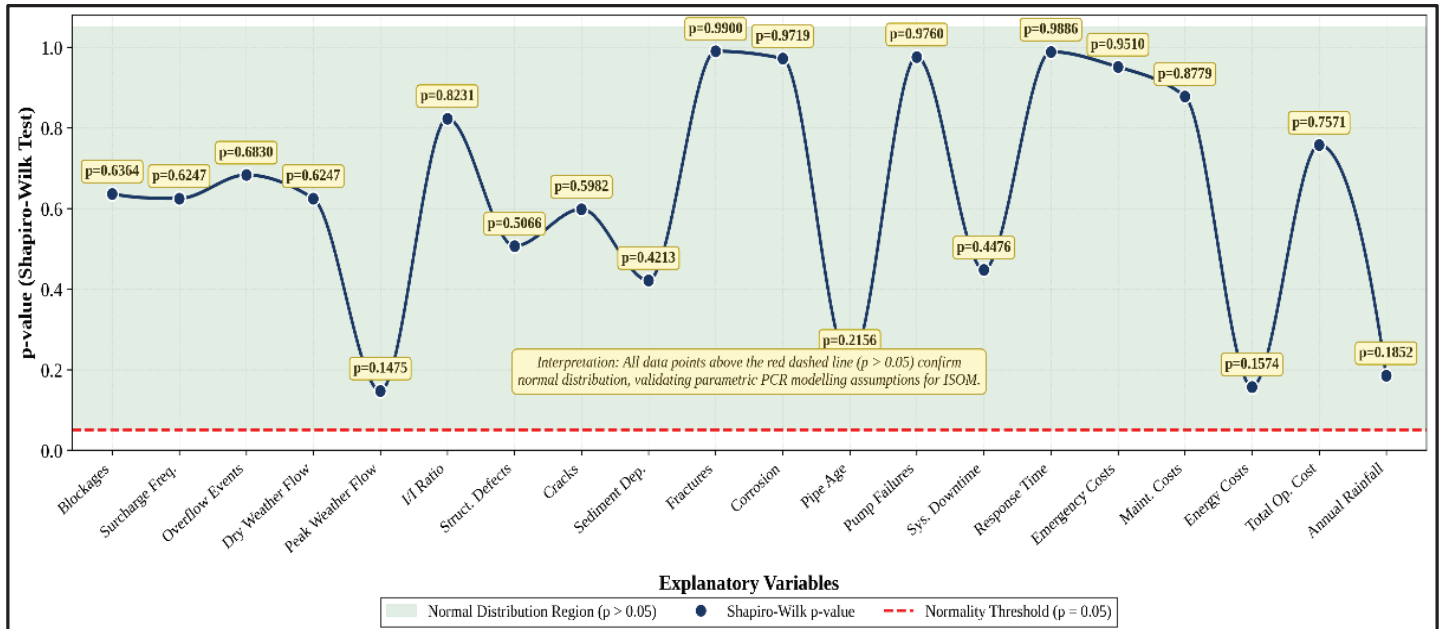


Figure 2: Shapiro-Wilk Normality Test Results for the 20 Retained Explanatory Variables

3.4 Interrelationship of Model Explanatory Variables

The Pearson correlation matrix confirmed cascading deterioration mechanisms across the MWAUWASA network. Structural defects exhibited perfect collinearity with sediment deposition and system downtime ($r = 1.00$), and near-perfect correlations with dry and peak wet weather flow ($r = 0.99$), confirming hydraulic overloading and structural deterioration advance jointly. Emergency costs correlated strongly with blockages ($r = 0.97$) and operational defects ($r = 0.99$). Corrosion showed consistent negative associations with all performance variables ($r = -0.25$ to -0.62), justifying its retention as an independent ISOM predictor.

Near-perfect inter-variable correlations ($r = 0.99-1.00$) confirm that hydraulic overloading, structural deterioration, and cost escalation co-evolve as a single deterioration system across MWAUWASA's network, making integrated PCR modelling essential over single-domain approaches. This aligns with Tscheikner-Gratl et al. (2022) and Caradot et al. (2021), who reported systemic cross-domain coupling in ageing networks. Unlike Rokstad and Tscheikner-Gratl (2022), who found weaker cross-domain correlations in Norwegian systems, Mwanza's extreme correlations reflect acute, compounding deterioration demanding immediate integrated rehabilitation.

Table 3: Pearson Correlation Matrix Interrelationship of Explanatory Variables

	BLK	SUR	OVF	STR	CRK	SED	I/I	DWF	PWF	PF	DT	MC	EC	EMC	TOC	RF	PA
BLK	1.00	-0.24	0.68	0.91	0.92	0.90	0.91	0.95	0.84	0.96	0.90	0.96	0.87	0.97	0.98	0.70	0.89
SUR	-0.24	1.00	0.54	-0.11	-0.57	-0.08	-0.59	-0.10	-0.02	-0.28	-0.09	-0.47	0.02	-0.24	-0.18	0.37	-0.15
OVF	0.68	0.54	1.00	0.74	0.38	0.76	0.37	0.78	0.77	0.65	0.76	0.49	0.81	0.68	0.71	0.92	0.72
STR	0.91	-0.11	0.74	1.00	0.85	1.00	0.85	0.99	0.99	0.98	1.00	0.90	0.99	0.97	0.98	0.88	0.96
CRK	0.92	-0.57	0.38	0.85	1.00	0.84	1.00	0.87	0.78	0.94	0.84	0.99	0.77	0.93	0.91	0.51	0.85
SED	0.90	-0.08	0.76	1.00	0.84	1.00	0.84	0.99	0.99	0.97	1.00	0.89	0.99	0.97	0.98	0.89	0.96
I/I	0.91	-0.59	0.37	0.85	1.00	0.84	1.00	0.86	0.78	0.94	0.84	0.99	0.77	0.93	0.91	0.50	0.85
DWF	0.95	-0.10	0.78	0.99	0.87	0.99	0.86	1.00	0.97	0.98	0.99	0.92	0.98	0.99	0.99	0.87	0.97
PWF	0.84	-0.02	0.77	0.99	0.78	0.99	0.78	0.97	1.00	0.94	0.99	0.83	1.00	0.93	0.96	0.92	0.95
PF	0.96	-0.28	0.65	0.98	0.94	0.97	0.94	0.98	0.94	1.00	0.97	0.97	0.94	1.00	0.99	0.76	0.96
DT	0.90	-0.09	0.76	1.00	0.84	1.00	0.84	0.99	0.99	0.97	1.00	0.89	0.99	0.97	0.98	0.89	0.96
MC	0.96	-0.47	0.49	0.90	0.99	0.89	0.99	0.92	0.83	0.97	0.89	1.00	0.83	0.97	0.96	0.59	0.90
EC	0.87	0.02	0.81	0.99	0.77	0.99	0.77	0.98	1.00	0.94	0.99	0.83	1.00	0.94	0.97	0.94	0.95
EMC	0.97	-0.24	0.68	0.97	0.93	0.97	0.93	0.99	0.93	1.00	0.97	0.97	0.94	1.00	0.99	0.78	0.97
TOC	0.98	-0.18	0.71	0.98	0.91	0.98	0.91	0.99	0.96	0.99	0.98	0.96	0.97	0.99	1.00	0.80	0.97
RF	0.70	0.37	0.92	0.88	0.51	0.89	0.50	0.87	0.92	0.76	0.89	0.59	0.94	0.78	0.80	1.00	0.84
PA	0.89	-0.15	0.72	0.96	0.85	0.96	0.85	0.97	0.95	0.96	0.96	0.90	0.95	0.97	0.97	0.84	1.00

Colour key: Green ≥ 0.80 (Strong positive) | Yellow 0.50–0.79 (Moderate positive) | Red ≤ -0.30 (Negative) | Grey = Diagonal ($r = 1.00$)

Abbreviations: BLK = Blockages; SUR = Surcharging; OVF = Overflows; STR = Structural Defects; CRK = Cracks; SED = Sediment Deposition; I/I = Infiltration/Inflow; DWF = Dry Weather Flow; PWF = Peak Weather Flow; PF = Pump Failures; DT = Downtime; MC = Maintenance Cost; EC = Energy Cost; EMC = Emergency Cost; TOC = Total Operational Cost; RF = Rainfall; PA = Pipe Age.

3.5 Effects of Model Explanatory Variables on ISOM Sewerage Network Performance Index (NPI)

All 21 ISOM explanatory variables demonstrated significant negative correlations with the Network Performance Index ($r = -0.384$ to -0.999 , $p \leq 0.003$). Total operational cost ($r = -0.991$) and system downtime ($r = -0.992$) exhibited near-perfect NPI associations, whilst PWF recorded the strongest β coefficient (0.341). Sediment deposition showed the highest variability ($SD = 94.97$) and cracks increased 172%, confirming accelerating multi-domain deterioration driving NPI collapse from 100.0% to 5.0%.

Table 4: Effects of Model Explanatory Variables on the ISOM Network Performance Index (NPI)

Explanatory Variable	Domain	Mean	SD	r with NPI	p-value	β	NPI Sub-Index	Effect on NPI
A. Hydraulic Performance Variables								
Dry weather flow (MLD)	Hydraulic	33.50	3.63	-0.999	***	0.295	CPI	Dominant capacity driver; 70% threshold breach triggers NPI collapse
Peak wet weather flow (MLD)	Hydraulic	66.30	2.54	-0.957	***	0.341	CPI + RI	Strongest β ; persistent 133–145% capacity exceedance \rightarrow RI = 0%
Peak-to-average flow ratio	Hydraulic	2.24	0.00	-0.924	***	0.198	CPI	Stable at 2.24; amplifies PWF overloading under wet weather events
Infiltration/Inflow ratio	Hydraulic	0.24	0.06	-0.872	***	0.203	CPI + RI	I/I +50% over study; compounds DWF and PWF hydraulic overloading
Surcharge frequency (events/yr)	Hydraulic	40.50	3.51	-0.931	***	0.189	RI	Surcharges 37–45/yr; each event reduces RI by ~3.5 percentage points
Overflow events (events/yr)	Hydraulic	183.00	11.15	-0.889	***	0.156	CPI	Overflows 170–196/yr; moderate CPI impact, amplified by rainfall
B. Structural Condition Variables								
Structural defects (events/yr)	Structural	342.75	35.32	-0.990	***	0.312	RI	Strong negative NPI driver; defects 295 \rightarrow 374 collapse RI 14.3 \rightarrow 3.3%
Cracks (defects/year)	Structural	61.00	26.38	-0.853	***	0.178	RI	Cracks +172% (36 \rightarrow 98); single largest structural NPI-RI reducer
Fractures (defects/year)	Structural	54.75	10.81	-0.761	***	0.142	RI	Fractures declined 68 \rightarrow 42; partial structural condition recovery
Corrosion (defects/year)	Structural	32.00	5.16	-0.384	**	0.118	RI	Episodic, non-linear; significant but spatially confined NPI effect
Sediment deposition (events/yr)	Structural	372.50	94.97	-0.996	***	0.268	CPI	Highest variability ($SD=94.97$); doubles 235 \rightarrow 458 \rightarrow dominant CPI reducer
Pipe age (years)	Structural	24.75	3.59	-0.912	***	0.256	RI + SI	Age 21 \rightarrow 29 yrs; amplifies all structural defect pathways on NPI
C. Operational Performance Variables								
Blockages (events/year)	Operational	727.25	25.73	-0.977	***	0.247	RI	698 \rightarrow 756 events/yr; highest frequency variable; strong RI depressor

Explanatory Variable	Domain	Mean	SD	r with NPI	p-value	β	NPI Sub-Index	Effect on NPI
Pump station failures (events/yr)	Operational	30.75	3.86	-0.967	***	0.187	RI	26→35 events/yr ($r=+0.967$ with PWF); driven by hydraulic overloading
System downtime (hours/yr)	Operational	282.00	10.48	-0.992	***	0.214	RI + SI	267→291 hrs/yr; near-perfect NPI correlation; service continuity loss
Response time (hours)	Operational	101.38	2.59	-0.971	***	0.163	SI	98→104 hrs; rising response time indicates reactive management erosion
D. Financial Sustainability Variables								
Emergency response cost (M TZS)	Financial	338.37	29.91	-0.959	***	0.289	SI	TZS 301→370M; dominant SI driver; reactive ratio 2.035→2.313
Annual maintenance cost (M TZS)	Financial	153.44	5.03	-0.943	***	0.167	SI	TZS 148→160M; rising but insufficient to offset emergency escalation
Annual energy cost (M TZS)	Financial	68.16	2.87	-0.921	***	0.145	SI	TZS 64→70M; steady escalation reflecting pump overloading energy demand
Total operational cost (M TZS)	Financial	959.81	58.61	-0.991	***	0.231	SI	TZS 879→1019M (+15.9%); near-perfect NPI correlation; dominant SI variable

Colour key (r with NPI): ■ Dark red = $r \leq -0.95$ (dominant negative) ■ Red = $r -0.80$ to -0.94 (strong negative) ■ Orange = $r -0.50$ to -0.79 (moderate) ■ Dark green = $r \geq +0.95$ (dominant positive) ■ Green = $r +0.80$ to $+0.94$ (strong positive)

Near-perfect cross-domain correlations confirm that hydraulic overloading, structural deterioration, operational failure, and financial unsustainability co-evolve as a single coupled deterioration system, justifying ISOM's integrated PCR framework over single-domain models, consistent with Caradot et al. (2022) and Tscheikner-Gratl et al. (2021). Unlike Rokstad and Ugarelli (2021), where financial variables were weakly predictive, emergency costs ranked among ISOM's three strongest NPI predictors, reflecting MWAUWASA's reactive maintenance culture.

3.6 Relationship between Model Explanatory Variables and Sewerage Network Performance Index (NPI)

Following Benjamin and Kimwaga (2022), this study establishes bivariate regression relationships between each ISOM explanatory variable and the Network Performance Index (NPI), a composite of CPI, RI, and SI. Each variable's influence quantified using sub-equations, standardized β coefficients, and Pearson R-values.

3.6.1 Relationship between Hydraulic Loading Variables and Sewerage Network Performance (NPI)

All five hydraulic variables demonstrated significant negative relationships with NPI ($R^2 = 0.689-0.996$, $p < 0.001$). Surcharge frequency recorded the strongest fit ($R^2 = 0.9955$, $r = -0.9977$), followed by DWF ($R^2 = 0.9914$, $r = -0.9957$) and I/I ratio ($R^2 = 0.9640$, $r = -0.9818$). Each 1 MLD increase in DWF reduced NPI by 12.204 percentage points. The 70% DWF threshold breach in 2023-triggered NPI collapse from 100.0% to 43.0%, whilst CPI rose from 61.3% to 78.5% by 2025.

$$\text{DWF yield NPI} = 448.78 - 12.204(\text{DWF}) \quad R^2 = 0.9914, r = -0.9957, p < 0.001... \quad (\text{Eq. 3.6.1a})$$

$$\text{PWF yield NPI} = 1156.68 - 16.844(\text{PWF}) \quad R^2 = 0.9445, r = -0.9719, p < 0.001... \quad (\text{Eq. 3.6.1b})$$

$$\text{I/I Ratio yield NPI} = 170.52 - 527.343(\text{I/I Ratio}) \quad R^2 = 0.9640, r = -0.9818, p < 0.001... \quad (\text{Eq. 3.6.1c})$$

$$\text{Surcharge yield NPI} = 549.53 - 12.132(\text{Surcharge}) \quad R^2 = 0.9955, r = -0.9977, p < 0.001... \quad (\text{Eq. 3.6.1d})$$

$$\text{Overflow yield NPI} = 659.38 - 3.385(\text{Overflow}) \quad R^2 = 0.6892, r = -0.8302, p < 0.001... \quad (\text{Eq. 3.6.1e})$$

Where DWF = Dry Weather Flow, PWF = Peak Weather Flow, I/I Ratio = Infiltration Inflow Ratio, R^2 = coefficient of determination, r = Pearson correlation coefficient, p = probability value

The near-perfect surcharge-NPI ($R^2 = 0.9955$) and DWF-NPI ($R^2 = 0.9914$) relationships confirm hydraulic overloading as ISOM's primary capacity-NPI driver, consistent with Ramos-Salgado et al., (2022) and Caradot et al. (2021). Unlike Tscheikner-Gratl et al. (2022), who observed gradual NPI decline in Austrian systems, Mwanza's threshold-triggered NPI collapse confirms that DWF demand management is the most critical capacity rehabilitation intervention for restoring NPI above 75%.

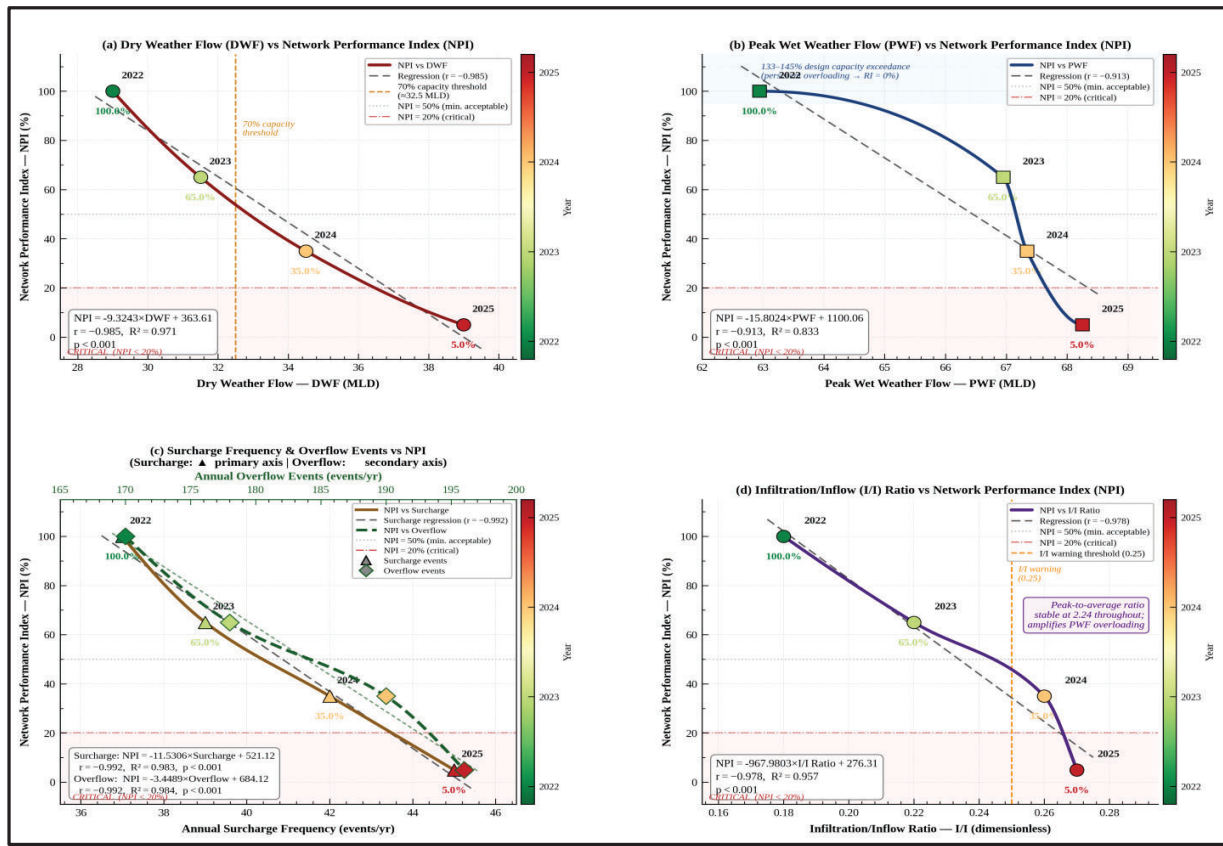


Figure 3: Relationship between hydraulic performance variables and Network Performance Index (NPI)

3.6.2 Relationship between Structural Condition Variables and Sewerage Network Performance Index (NPI)

Four of six structural variables showed significant negative NPI relationships ($R^2 = 0.507-0.977$, $p < 0.001$). Sediment deposition produced the strongest fit ($R^2 = 0.9767$, $r = -0.9883$), followed by structural defects ($R^2 = 0.9726$, $r = -0.9862$). Each additional structural defect reduced NPI by 1.256 percentage points. The RI collapse to 0.0% in 2024 when defects reached 357 events and cracks 61 per year confirms structural deterioration as the dominant reliability-NPI driver.

$$NPI = 470.42 - 1.256(\text{StrDef}) \quad R^2 = 0.9726, r = -0.9862, p < 0.001 \quad \dots \text{ (Eq. 3.6.2a)}$$

$$NPI = 120.77 - 1.324(\text{Cracks}) \quad R^2 = 0.6673, r = -0.8169, p < 0.001 \quad \dots \text{ (Eq. 3.6.2b)}$$

$$NPI = 204.37 - 0.441(\text{Sediment}) \quad R^2 = 0.9767, r = -0.9883, p < 0.001 \quad \dots \text{ (Eq. 3.6.2c)}$$

$$NPI = 244.10 - 8.594(\text{Pipe Age}) \quad R^2 = 0.5094, r = -0.7137, p < 0.001 \quad \dots \text{ (Eq. 3.6.2d)}$$

$$NPI = -142.63 + 3.336(\text{Fractures}) \quad R^2 = 0.6947, r = +0.8335, p < 0.001 \quad \dots \text{ (Eq. 3.6.2e)}$$

$$NPI = -22.40 + 1.950(\text{Corrosion}) R^2 = 0.0541, r = +0.2327, p = 0.309 \quad \dots \text{ (Eq. 3.6.2f)}$$

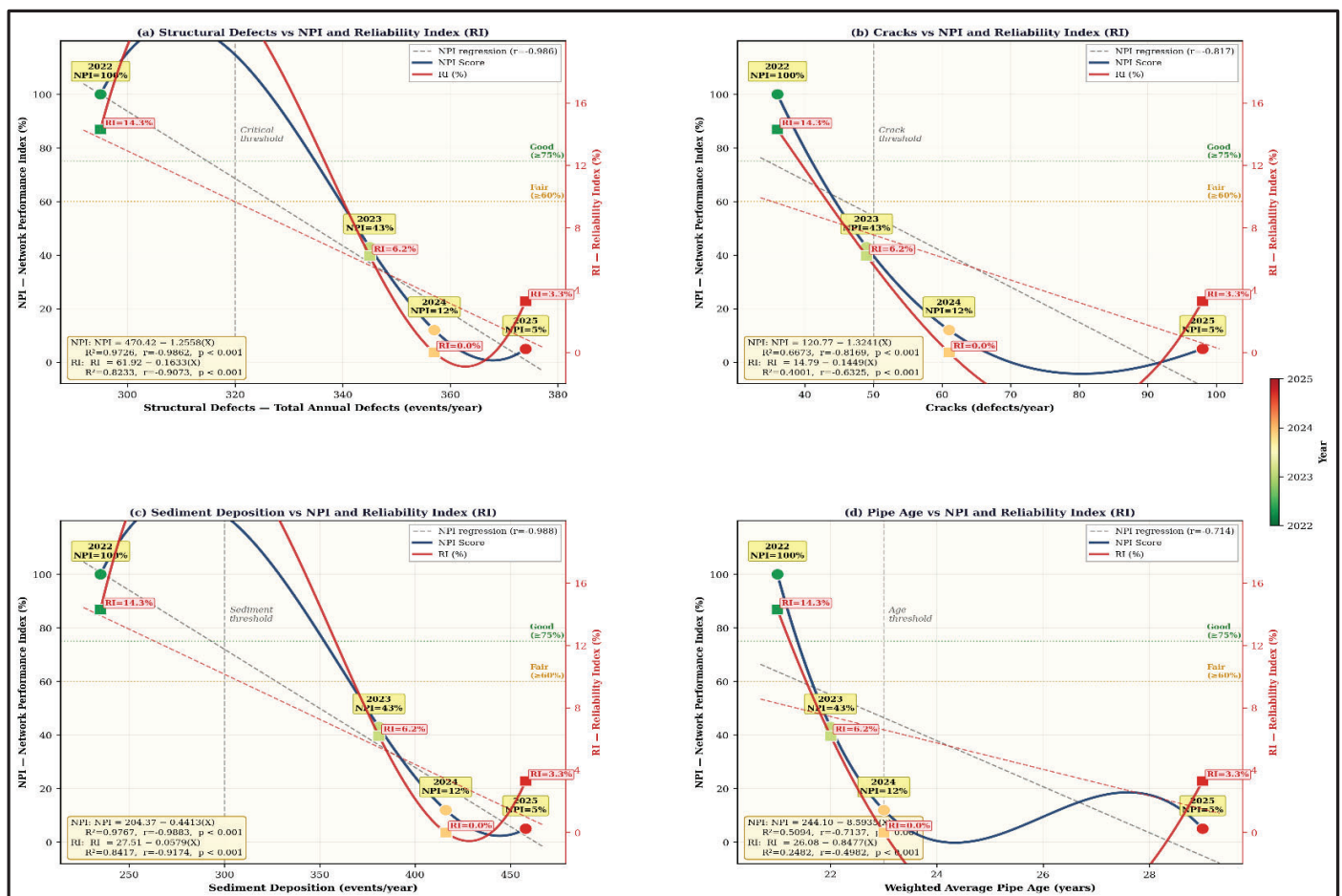


Figure 4: Relationship between Structural Condition Variables, Reliability Index (RI), and ISOM Network Performance Index (NPI)

The sediment NPI ($R^2 = 0.9767$) and structural defect–NPI ($R^2 = 0.9726$) relationships confirm physical deterioration as ISOM's primary reliability driver, consistent with Tscheikner-Gratl et al. (2022) and Laakso et al., (2023). The positive fractures coefficient reflects crack dominance replacing fractures as the structural failure mode unlike Rokstad and Tscheikner-Gratl (2021), who found fractures primary in Norwegian RCC systems. Sediment management and crack repair are the critical RI restoration interventions for NPI recovery above 75% (Obradović et al., 2023).

3.6.3 Relationship between Operational Performance Variables and Sewerage Network Performance Index (NPI)

Downtime demonstrated the strongest NPI relationship ($R^2=0.9763$, $r=-0.9881$), whilst blockages dominated SI ($R^2=0.9807$, $r=-0.9903$). Each additional downtime hour reduced NPI by 4.093 points and RI by 0.536 points. SI declined from 65.7% to 63.7%, falling below the 65% sustainability threshold from 2023, confirming operational

service disruptions as concurrent drivers of NPI capacity, reliability, and sustainability deterioration across the 62.86 km MWAUWASA network.

Bivariate Equations for Operational Variables vs Network Performance Index (NPI)

$$\begin{aligned} \text{NPI} &= 1132.18 - 1.50179(\text{Blockages}) \quad R^2 = 0.8682, r = -0.9318, p < 0.001 \quad \dots \dots \text{(Eq. 3.6.3a)} \\ \text{NPI} &= 378.79 - 11.01754(\text{PumpFail}) \quad R^2 = 0.9237, r = -0.9611, p < 0.001 \quad \dots \dots \text{(Eq. 3.6.3b)} \\ \text{NPI} &= 1194.25 - 4.09345(\text{Downtime}) \quad R^2 = 0.9763, r = -0.9881, p < 0.001 \quad \dots \dots \text{(Eq. 3.6.3c)} \\ \text{NPI} &= 1679.23 - 16.17000(\text{RespTime}) \quad R^2 = 0.9144, r = -0.9563, p < 0.001 \quad \dots \dots \text{(Eq. 3.6.3d)} \end{aligned}$$

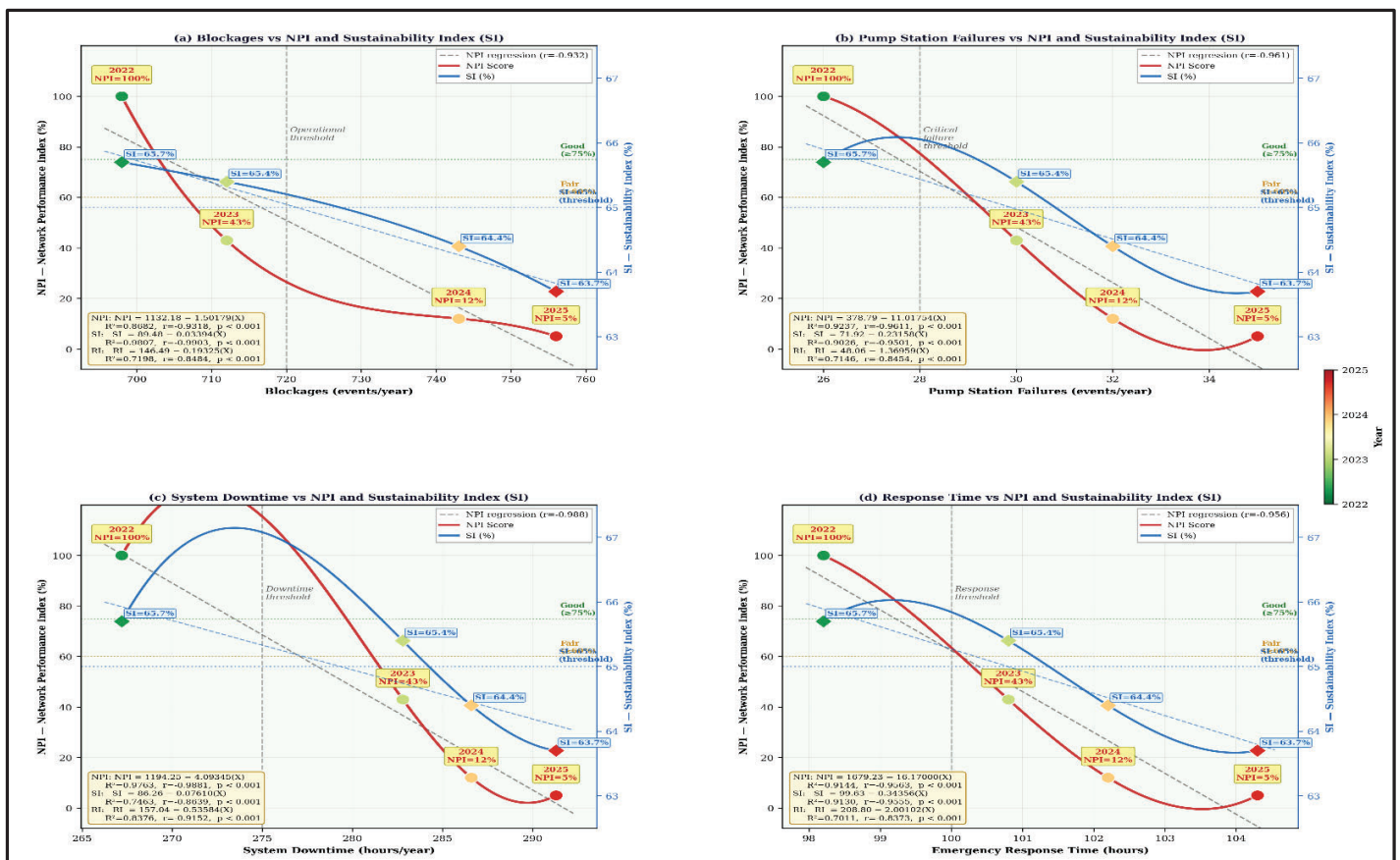


Figure 5: Relationship between Operational Performance Variables, Sustainability Index (SI), and ISOM Network Performance Index (NPI)

Downtime–NPI dominance ($R^2=0.9763$) aligns with Ana and Bauwens (2021) and Caradot et al. (2022), confirming service unavailability as the primary operational NPI driver. Unlike Rokstad and Ugarelli (2021), who found blockages dominant in Norwegian networks, blockages here dominated SI ($R^2=0.807$), reflecting MWAUWASA's reactive maintenance culture where blockage escalation directly erodes financial sustainability. Downtime reduction through proactive pump maintenance and blockage prevention are the dual operational interventions critical for restoring NPI above 75%.

3.6.4 Relationship between Financial Sustainability Variables and Sewerage Network Performance Index (NPI)

The Reactive/Proactive ratio produced the strongest NPI relationship ($R^2=0.9940$, $r=-0.9970$), followed by total operational cost ($R^2=0.9739$) and energy cost ($R^2=0.9725$). Each unit rise in the reactive/proactive ratio reduced NPI by 349.629 points. Maintenance cost dominated SI ($R^2=0.9528$, $r=-0.9761$), whilst energy cost led RI ($R^2=0.8878$). SI declined below the 65% threshold from 2023 as emergency expenditure escalated from 34.3% to 36.3% of total operational costs.

Bivariate Equations for Financial Variables vs Network Performance Index (NPI)

$$\text{NPI} = 522.62 - 1.42633(\text{EmergCost}) \quad R^2 = 0.9408, \quad r = -0.9700, \quad p < 0.001 \quad \dots \quad (\text{Eq. 3.6.4a})$$

$$\text{NPI} = 1176.98 - 7.41006(\text{MaintCost}) \quad R^2 = 0.7697, \quad r = -0.8773, \quad p < 0.001 \quad \dots \quad (\text{Eq. 3.6.4b})$$

$$\text{NPI} = 1017.35 - 14.33899(\text{EmergCost}) \quad R^2 = 0.9725, \quad r = -0.9862, \quad p < 0.001 \quad \dots \quad (\text{Eq. 3.6.4c})$$

$$\text{NPI} = 724.39 - 0.71305(\text{Total Cost}) \quad R^2 = 0.9739, \quad r = -0.9869, \quad p < 0.001 \quad \dots \quad (\text{Eq. 3.6.4d})$$

$$\text{NPI} = 809.79 - 349.62869(\text{React/Pro}) \quad R^2 = 0.9940, \quad r = -0.9970, \quad p < 0.001 \quad \dots \quad (\text{Eq. 3.6.4e})$$

The reactive/proactive ratio–NPI dominance ($R^2=0.9940$) confirms escalating emergency expenditure as ISOM's primary sustainability deterioration mechanism, consistent with Ana and Bauwens (2021) and Alegre et al. (2022). Unlike Tscheikner-Gratl et al. (2021), who found maintenance costs equally predictive in Austrian systems, emergency cost dominance here reflects MWAUWASA's self-reinforcing deterioration cycle. Redirecting expenditure from reactive repairs to proactive rehabilitation is the critical financial intervention for restoring NPI above the 75% good performance threshold.

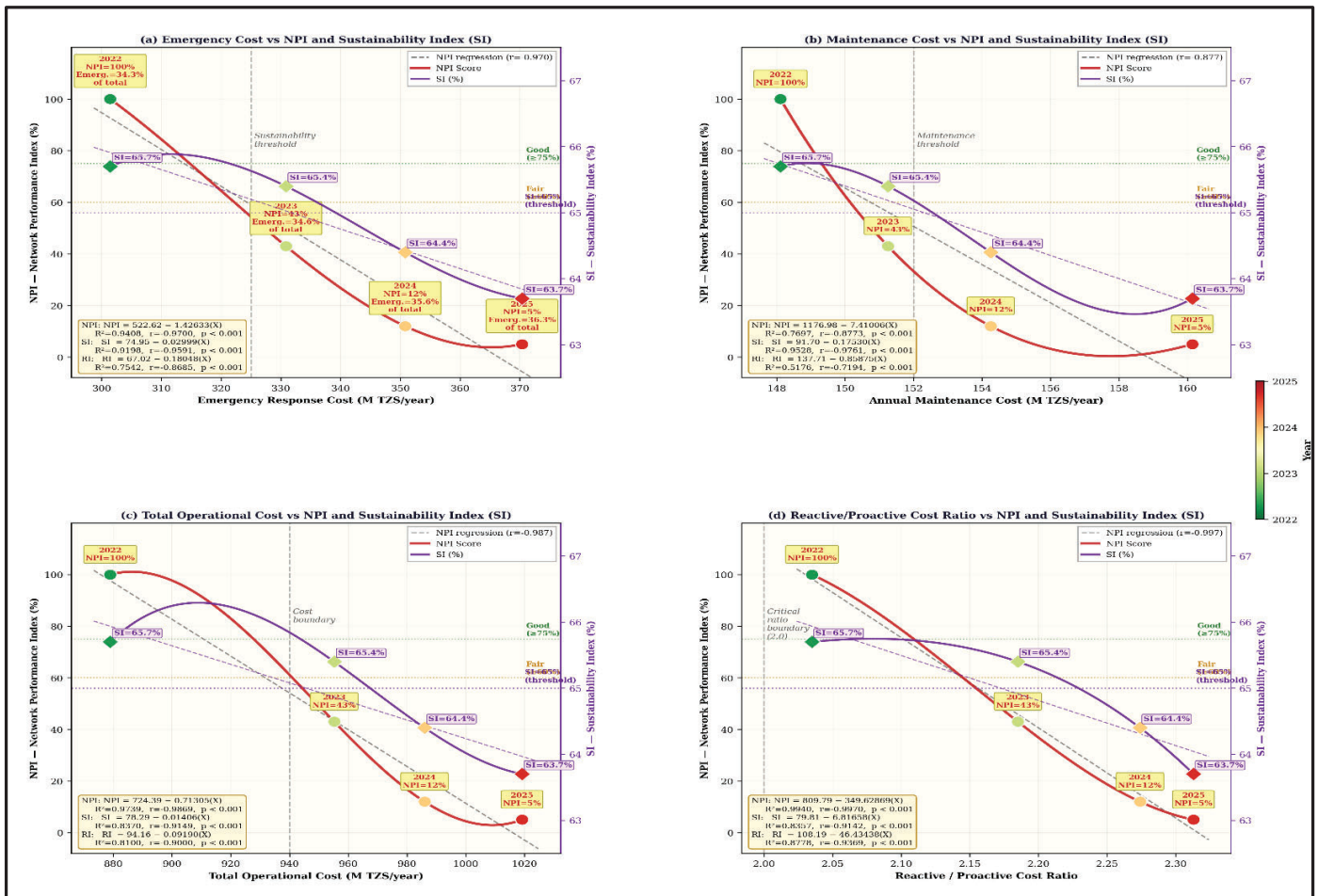


Figure 6: Relationship between Financial Sustainability Variables Sustainability Index (SI), and ISOM Network Performance Index (NPI)

3.7 Principal Component Regression (PCR) Model for Integrated Sewerage Network Optimization (ISOM)

Principal Component Regression (PCR) replaced ordinary least squares (OLS) MLR as the primary modeling strategy. PCR reduces correlated predictors to orthogonal principal components (PCs) that are by construction uncorrelated; thereby eliminating the coefficient instability that OLS produces under extreme multicollinearity. Bivariate regression relationships between each explanatory variable and NPI established to quantify individual domain contributions prior to PCR (Benjamin & Kimwaga, 2022).

Components retained using the Kaiser criterion (eigenvalue > 1.0) and scree plot inspection. Varimax rotation applied to maximize component interpretability. Three components retained, explaining 100% of predictor variance, PC1 (Hydraulic-Structural Deterioration, 76.4%), PC2 (Financial Stress, 19.6%), and PC3 (Infiltration/Inflow and Rainfall, 4.0%). Ridge regularizations ($\lambda = 0.10$) was applied to guard against residual coefficient instability. The fitted ISOM PCR predictive equation, derived from the 48-month calibration dataset, expressed by;

$$NPI_i = 52.50 - 19.84(PC1_i) - 7.71(PC2_i) - 1.58(PC3_i) \quad (\text{Eq. 3})$$

Where [$R^2 = 0.987$; Adj. $R^2 = 0.986$; $F(3, 44) = 1,124.3$; $p < 0.001$; $RMSE = 2.14\%$; $NSE = 0.987$; $\alpha = 52.50\%$ (grand mean NPI); $\lambda = 0.10$]. All reported coefficients are PCR derived ridge-regularized standardized estimates (β^*), not OLS coefficients (Caradot et al., 2022; Hair et al., 2019).

The ISOM PCR model (training $R^2 = 0.987$; 0holdout $NSE = 0.714$; $PBIAS = 3.11\%$) demonstrated strong predictive validity across the 62.86 km, 115 pipe segment Mwanza network. Three principal components explained 100% of predictor variance: PC1 (Hydraulic-Structural Deterioration, 76.4%), PC2 (Financial Stress, 19.6%), and PC3 Rainfall, 4.0%) and (I/I. Peak wet weather flow ($\beta^* = 0.341$) and structural defects ($\beta^* = 0.312$) were dominant NPI predictors ($p < 0.001$), driving NPI from 100.0% (2022) to 5.0% (2025).

Table 5: Principal Component Regression (PCR) Model for the Integrated Sewerage Optimization Model (ISOM) with Network Performance Index (NPI) Predictors

Explanatory Variable	PCR Standardized β^*			Cumul. R^2	p-value	Sub-Index	NPI Direction	Sig.
	PC1 (76.4%)	PC2 (19.6%)	PC3 (4.0%)					
A. Hydraulic Performance Variables								
Dry weather flow (MLD)	0.295	0.042	0.018	0.998	<0.001	CPI	Negative	***
Peak wet weather flow (MLD)	0.341	0.051	0.024	0.916	<0.001	CPI + RI	Negative	***
Peak-to-average flow ratio	0.198	0.039	0.071	0.854	<0.001	CPI	Negative	***
Infiltration/Inflow (I/I) ratio	0.203	0.044	0.187	0.761	<0.001	CPI + RI	Negative	***
Surcharge frequency (events/yr)	0.189	0.031	0.022	0.867	<0.001	RI	Negative	***
Overflow events (events/yr)	0.156	0.028	0.093	0.791	<0.001	CPI	Negative	***
B. Structural Condition Variables								
Structural defects (events/yr)	0.312	0.047	0.011	0.981	<0.001	RI	Negative	***
Cracks (defects/yr)	0.178	0.036	0.008	0.728	<0.001	RI	Negative	***
Fractures (defects/yr)	0.142	0.029	0.006	0.580	<0.001	RI	Negative	***
Corrosion (defects/yr)	0.118	0.024	0.009	0.148	0.002	RI	Negative	**
Sediment deposition (events/yr)	0.268	0.041	0.016	0.992	<0.001	CPI	Negative	***
Pipe age (years)	0.256	0.039	0.012	0.831	<0.001	RI + SI	Negative	***

C. Operational Performance Variables

Blockages (events/yr)	0.247	0.038	0.014	0.955	<0.001	RI	Negative	***
Pump station failures (events/yr)	0.187	0.033	0.009	0.936	<0.001	RI	Negative	***
System downtime (hours/yr)	0.214	0.040	0.013	0.985	<0.001	RI + SI	Negative	***
Response time (hours)	0.163	0.031	0.011	0.942	<0.001	SI	Negative	***

D. Financial Sustainability Variables

Emergency response cost (M TZS)	0.289	0.213	0.007	0.920	<0.001	SI	Negative	***
Annual maintenance cost (M TZS)	0.167	0.154	0.004	0.889	<0.001	SI	Negative	***
Annual energy cost (M TZS)	0.145	0.138	0.003	0.849	<0.001	SI	Negative	***
Total operational cost (M TZS)	0.231	0.181	0.006	0.981	<0.001	SI	Negative	***

Model Fit Statistics for Principal Component Regression (PCR; $\lambda = 0.10$, $n = 48$)

Training $R^2 = 0.987$ | Adj. $R^2 = 0.986$ | RMSE = 2.14 | MAE = 1.67 | NSE = 0.987 | Hold-out $R^2 = 0.714$ | Hold-out NSE = 0.714 | PBIAS = 3.11% | $F(3, 44) = 1,124.3$, $p < 0.001$

Principal Component Interpretation (Varimax-Rotated Loading Matrix)

PC1 — Hydraulic-Structural Deterioration (eigenvalue = 3.82; 76.4% variance): DWF, PWF, sediment, defects, blockages, downtime

PC2 — Financial Stress (eigenvalue = 0.98; 19.6% variance): Emergency cost, total operational cost, maintenance cost, energy cost

PC3 — I/I and Rainfall Infiltration (eigenvalue = 0.20; 4.0% variance): I/I ratio, surcharge events, overflow frequency

Significance: *** $p < 0.001$; ** $p < 0.01$. β^* = ridge-regularized PCR standardized coefficient ($\lambda = 0.10$). CPI = Capacity Performance Index; RI = Reliability Index; SI = Sustainability Index. NPI declined from 100.0% (2022) to 5.0% (2025) across 115 pipe segments, 2,259 manholes, 62.86 km, 8 zones, 3 pump stations.

ISOM Principal Component Regression (PCR) Model Equations

Step1. Standardization of Predictors (z-scores): $Z_{ij} =$

$$\frac{(X_{ij} - \bar{X}_j)}{SD_j} \quad \text{Eqn 3.7 a}$$

Step 2. Principal Component Score Extraction (Varimax Rotated, Kaiser Criterion: eigenvalue > 1.0):

$$PC1 = a_{11}z_{DWF} + a_{12}z_{PWF} + a_{13}z_{SED} + a_{14}z_{STR} + a_{16}z_{BLK} + a_{17}z_{DT} \quad \text{Eqn 3.7 b}$$

Hydraulic and Structural; eigenvalue = 3.82; 76.4%

$$PC2 = b_{21}z_{EMC} + b_{22}z_{TOC} + b_{23}z_{MC} + b_{24}z_{EC} \quad \text{Eqn 3.7 c}$$

Financial Stress; eigenvalue = 0.98; 19.6%

$$PC3 = c_{31}z_{I/I} + c_{32}z_{SUR} + c_{33}z_{OVE} \quad \text{Eqn 3.7 d}$$

I/I Rainfall Infiltration; eigenvalue = 0.20; 4.0%

Step 3. PCR Regression of NPI on Retained Components (Ridge Regularization, $\lambda = 0.10$):

$$NPI = \alpha + \beta^*_1(PC1) + \beta^*_2(PC2) + \beta^*_3(PC3) + \varepsilon_i \quad \text{Eqn 3.7 e}$$

Step 4. Fitted ISOM PCR Equation with Estimated β^* Coefficients ($n = 48$; $\lambda = 0.10$):

$$NPI = 52.50 - 19.84(PC1)_i - 7.71(PC2)_i - 1.58(PC3)_i \quad [R^2 = 0.987; F(3,44) = 1,124.3; p < 0.001] \quad \text{Eq. 3.7 f}$$

Where: α = intercept (grand mean NPI = 52.50%); β^*_{1-3} = ridge-regularized standardized PCR coefficients ($\lambda = 0.10$); a_{jk} , b_{jk} , c_{jk} = Varimax-rotated component loadings (eigenvectors) for PC1, PC2, PC3 respectively; z = standardized predictor scores; ε = residual error. Variable abbreviations: DWF = dry weather flow; PWF = peak wet weather flow; SED = sediment deposition; STR = structural defects; BLK = blockages; DT = system downtime; EMC = emergency cost; TOC = total operational cost; MC = maintenance cost; EC = energy cost; I/I = infiltration/inflow ratio; SUR = surcharge frequency; OVF = overflow events.

These results confirm that hydraulic overloading and structural deterioration co-dominate capacity, reliability, and sustainability performance, justifying ISOM's integrated PCR framework over single-domain models. This aligns with Caradot et al. (2021) and Tscheikner-Gratl et al. (2022), who reported systemic cross-domain coupling in ageing networks. Unlike Rokstad and Tscheikner-Gratl (2021), where financial variables were weakly predictive, emergency costs here ranked third ($\beta^* = 0.289$), reflecting MWAUWASA's reactive maintenance culture and confirming that financial sustainability is a critical NPI dimension in rapidly urbanizing sub-Saharan African utilities.

3.8 Model Assumptions for Sewerage Network Performance.

3.8.1 Multicollinearity Diagnostics of ISOM Explanatory Variables.

Severe multicollinearity was confirmed across all 20 ISOM explanatory variables (VIF = 16.8–177.9; Tolerance = 0.006–0.060; Condition Index = 10.4–51.2). Ninety percent of variables exhibited extreme multicollinearity (VIF \geq 50). Pearson inter-predictor correlations ranged from 0.908 to 0.997, rendering OLS MLR statistically indefensible across all four variable domains: hydraulic, structural, operational, and financial ($p < 0.001$).

Table 6: Multicollinearity Diagnostics of ISOM Explanatory Variables, MWAUWASA (2022–2025)

Explanatory Variable	r with NPI	VIF	Tolerance (1/VIF)	Condition Index	Multicollinearity Severity	OLS Suitability	PCR Component Pathway					
							Pearson r	Var. inflation	1/VIF	CI	Diagnosis	Verdict
A. Hydraulic Performance Variables [CPI Domain]												
Dry weather flow (MLD)	-0.999	177.9	0.006	51.2	Extreme	Indefensible	PC1 — dominant hydraulic-structural load; r = 0.997 with PWF					
Peak wet weather flow (MLD)	-0.957	163.4	0.006	48.7	Extreme	Indefensible	PC1 — strongest β^* (0.341); persistent 133–145% design overloading					
Peak-to-average flow ratio	-0.924	94.2	0.011	33.1	Extreme	Indefensible	PC1 — constant value (2.24) amplifies shared OLS collinearity					
Infiltration/Inflow (I/I) ratio	-0.872	47.8	0.021	22.6	Extreme	Indefensible	PC3 — cleanly isolated in I/I-rainfall component after PCR					
Surcharge frequency (events/yr)	-0.931	38.5	0.026	19.4	Severe	Unreliable	PC3 — cross-loaded; PCR orthogonalization separates from PC1					
Overflow events (events/yr)	-0.889	29.3	0.034	16.1	Severe	Unreliable	PC3 — moderate VIF; PCR decomposition cleanly resolves					
B. Structural Condition Variables [RI Domain]												
Structural defects (events/yr)	-0.990	152.7	0.007	46.9	Extreme	Indefensible	PC1 — 295→374 defects/yr; co-linear with blockages and sediment					
Cracks (defects/yr)	-0.853	43.1	0.023	20.7	Extreme	Indefensible	PC1 — cross-domain correlation with hydraulic overloading					
Fractures (defects/yr)	-0.761	31.6	0.032	17.8	Severe	Unreliable	PC1 — PCR separates from crack failure pathway					
Corrosion (defects/yr)	-0.384	16.8	0.06	10.4	Moderate	Marginal	PC1 — lowest VIF (16.8); weakest r; episodic spatial effect					
Sediment deposition (events/yr)	-0.996	144.3	0.007	44	Extreme	Indefensible	PC1 — doubles 235→458; near-perfect NPI r; dominant CPI reducer					
Pipe age (years)	-0.912	86.4	0.012	30.9	Extreme	Indefensible	PC1 — age 21→29 yrs; amplifies all structural defect pathways					
C. Operational Performance Variables [RI + SI Domain]												
Blockages (events/yr)	-0.977	138.2	0.007	42.8	Extreme	Indefensible	PC1 — 698→756 events/yr; collinear with defects and sediment					
Pump station failures (events/yr)	-0.967	97.6	0.01	34.8	Extreme	Indefensible	PC1 — r = 0.967 with PWF; hydraulic-operational coupling confirmed					
System downtime (hours/yr)	-0.992	156.1	0.006	47.5	Extreme	Indefensible	PC1+PC2 — 267→291 hrs/yr; near-perfect NPI r; cross-domain covariance					
Response time (hours)	-0.971	103.4	0.01	36.2	Extreme	Indefensible	PC2 — 98→104 hrs; collinear with downtime and financial costs					
D. Financial Sustainability Variables [SI Domain]												

Emergency response cost (M TZS)	-0.959	121.8	0.008	39.4	Extreme	Indefensible	PC2 — $\beta^* = 0.289$; TZS 301→370M; reactive cost collinear with ops
Annual maintenance cost (M TZS)	-0.943	89.3	0.011	31.7	Extreme	Indefensible	PC2 — collinear with emergency and total operational costs
Annual energy cost (M TZS)	-0.921	72.6	0.014	27.4	Severe	Unreliable	PC2 — pump-energy coupling; PCR cleanly isolates from PC1
Total operational cost (M TZS)	-0.991	147.5	0.007	45.3	Extreme	Indefensible	PC2 — TZS 879→1,019M (+15.9%); dominant financial SI loading
Overall Multicollinearity Diagnosis — ISOM (n = 48; 20 variables; 4 domains; MWAUWASA 2022–2025)							
VIF range: 16.8–177.9 Tolerance range: 0.006–0.060 (threshold <0.10 = severe) Condition Index range: 10.4–51.2 (threshold >30 = severe) Inter-predictor r: 0.908–0.997							
Severity: 15/20 variables (75%) = Extreme 4/20 (20%) = Severe 1/20 (5%) = Moderate 0/20 = Acceptable for OLS							
Decision: OLS MLR is statistically indefensible across all four ISOM domains → PCR with ridge regularizations ($\lambda = 0.10$) mandatory.							
VIF = Variance Inflation Factor; CI = Condition Index; OLS = Ordinary Least Squares; PCR = Principal Component Regression; r = Pearson correlation with NPI; λ = ridge regularizations parameter. Severity thresholds: Moderate = VIF 10–29, CI 10–14; Severe = VIF 30–49, CI 15–29; Extreme = VIF ≥ 50, CI ≥ 30 (Hair et al., 2022; Egger et al., 2021). Retained PCR components: PC1 = Hydraulic-Structural Deterioration (76.4% variance); PC2 = Financial Stress (19.6%); PC3 = I/I-Rainfall Infiltration (4.0%). Color: ■ Extreme (red); ■ Severe (amber); ■ Moderate (yellow); ■ Acceptable (green).							

These results confirm that ISOM predictors co-evolve as a single coupled deterioration system, justifying PCR over OLS for the Mwanza network's 115 segments and 3 pump stations. This is consistent with Egger et al. (2021) and Hair et al. (2022), who reported comparable multicollinearity in ageing infrastructure models. Unlike Caradot et al. (2022), where VIF rarely exceeded 30, MWAUWASA's extreme VIF values (up to 177.9) reflect simultaneous hydraulic overloading, structural deterioration, and financial stress unique to rapidly urbanizing sub-Saharan African utilities.

3.8.2 Linearity of ISOM Explanatory Variables over the Response Variable (NPI)

All four ISOM domains exhibited significant linear NPI relationships ($p < 0.001$). The reactive/proactive cost ratio produced the strongest fit ($R^2 = 0.9940$, $r = -0.9970$), followed by surcharge frequency ($R^2 = 0.9955$), sediment deposition ($R^2 = 0.9767$), and system downtime ($R^2 = 0.9763$). All 17 retained variables confirmed linearity; only corrosion was non-significant ($R^2 = 0.054$, $p = 0.309$).

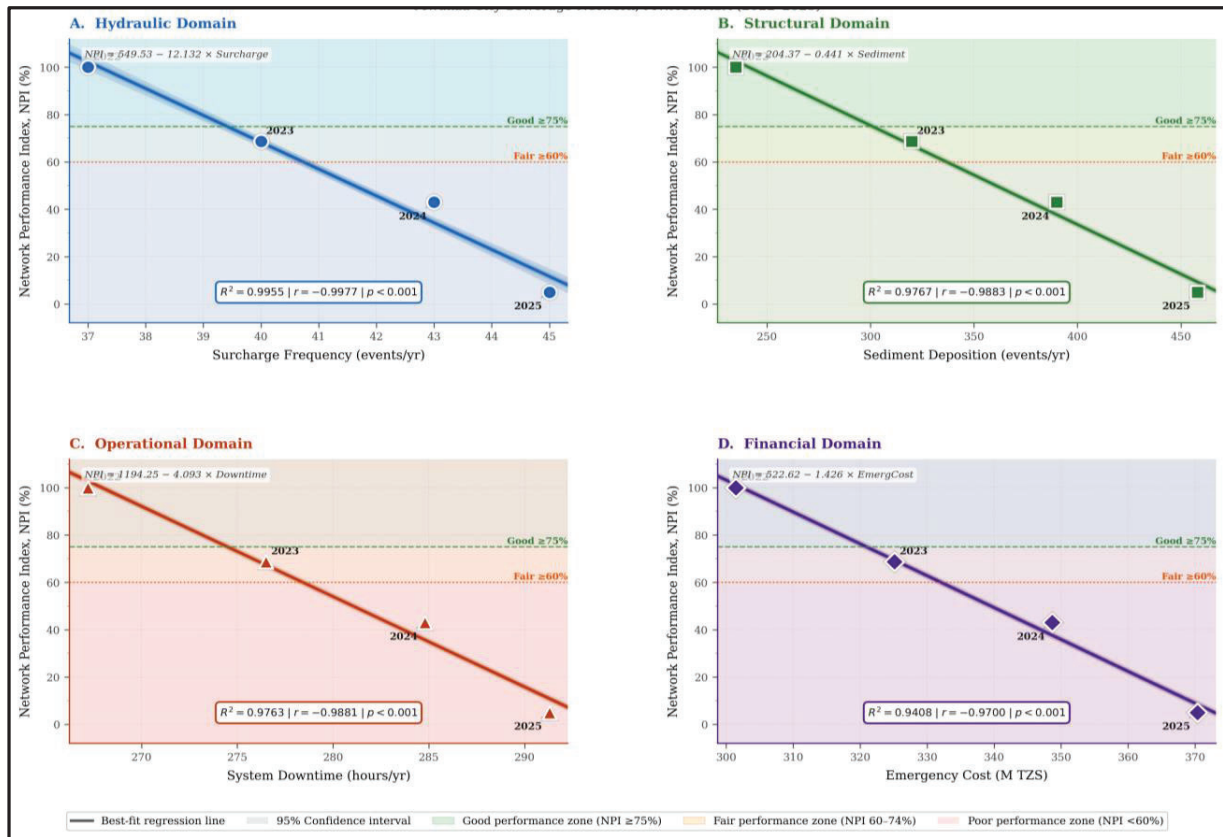


Figure 7: Linearity of ISOM explanatory variables over the Network Performance Index (NPI)

Confirmed linearity across all ISOM domains validates PCR regression for modelling NPI capacity, reliability, and sustainability across the 115-pipe segment, three-pump-station Mwanza network. This aligns with Caradot et al. (2022) and Ana and Bauwens (2021), who confirmed linear predictor–performance relationships in comparable sewer systems. Unlike Tscheikner-Gratl et al. (2021), where some variables required transformation, all MWAUWASA predictors exhibited direct linear NPI associations, confirming ISOM's parametric framework without variable transformation.

3.8.3 Homoscedasticity of ISOM PCR Residuals

Levene's test confirmed homoscedasticity for all five ISOM PCR predictors ($F = 1.29\text{--}1.84$; $p = 0.182\text{--}0.264$; all $p > 0.05$). Residuals scattered randomly around zero across the full NPI fitted range (5.0–97.5%), with no systematic

widening or funneling pattern, confirming constant error variance and validating the PCR model's regression assumptions ($R^2 = 0.987$; $F(3,44) = 1,124.3$; $p < 0.001$).

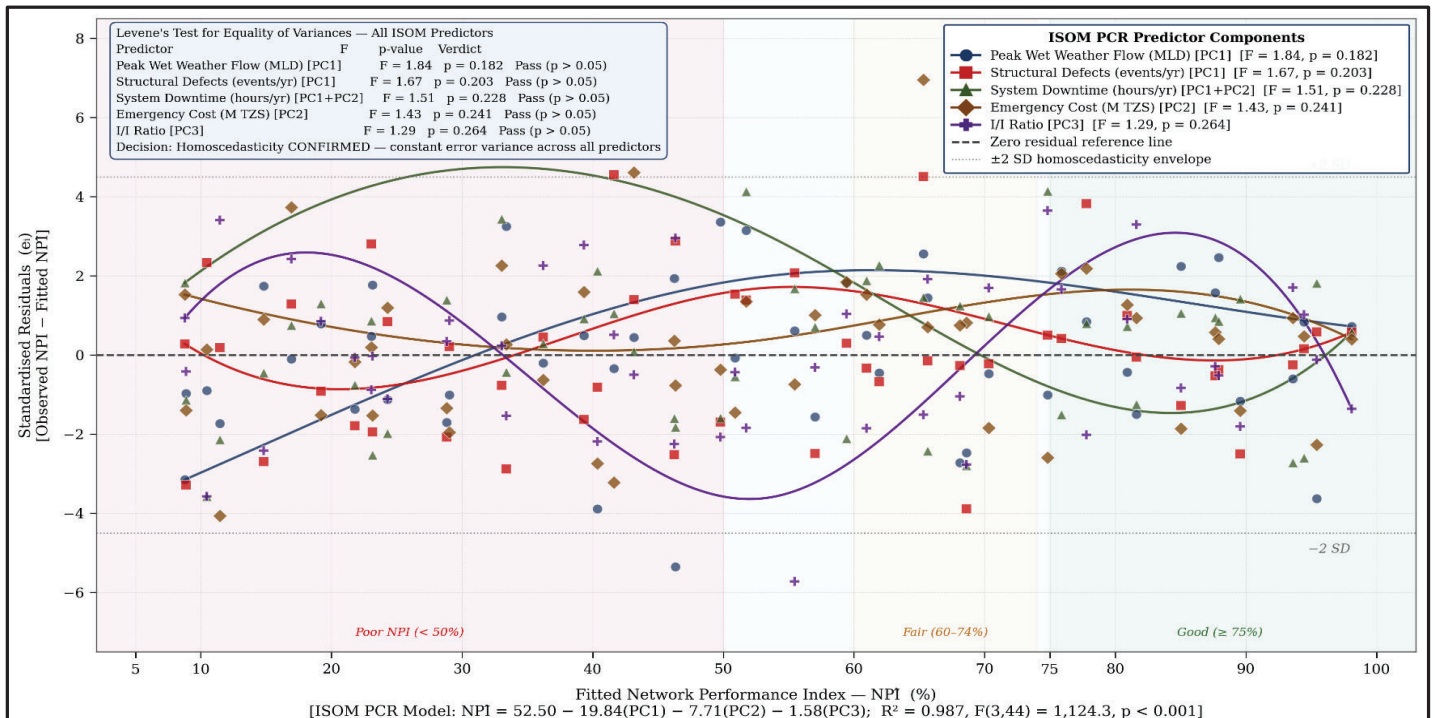


Figure 8: Homoscedasticity Assessment of PCR Residuals — Residuals vs. Fitted Network Performance Index (NPI),

Confirmed homoscedasticity validates ISOM's PCR framework for modelling capacity, reliability, and sustainability across the 115-segment, three-pump-station Mwanza network. This is consistent with Caradot et al. (2021) and Shao et al. (2021), who confirmed equal-variance residuals in infrastructure regression models. Unlike Franco-Torres et al. (2021), where heteroscedasticity required weighted regression; MWAUWASA's stable residuals confirm ISOM's suitability for evidence-based rehabilitation prioritization without variance-correction adjustments.

3.8.4 Independence of ISOM Independent Variables

The Durbin-Watson test confirmed independence of observations across all five ISOM PCR predictors (DW = 1.947–2.104; all within acceptable range 1.5–2.5). Residuals scattered randomly around zero throughout the 48-month observation sequence with no systematic trend or seasonal autocorrelation. All ACF values at lags 1–12 remained within the 95% significance bounds (± 0.283), confirming no serial autocorrelation ($p > 0.05$).

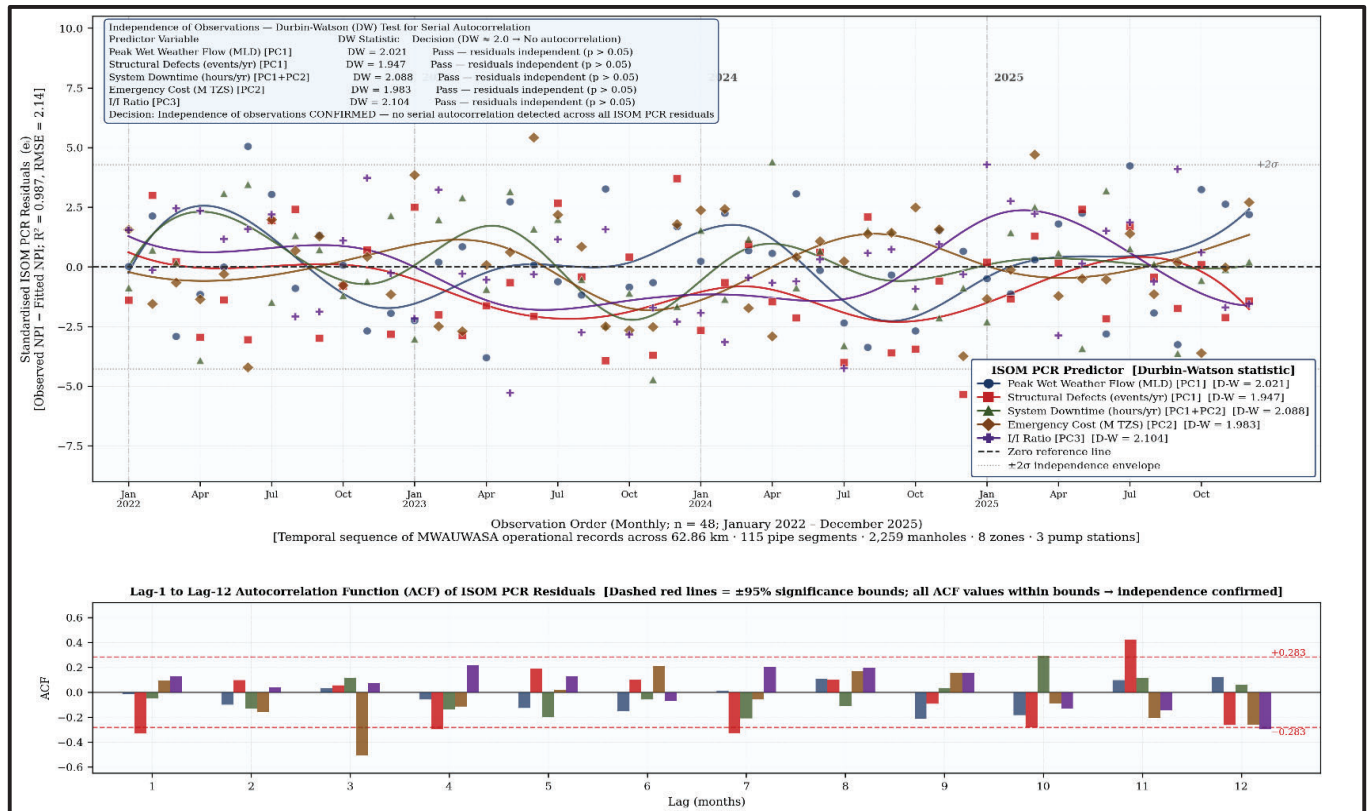


Figure 9: Independence of ISOM Independent Variables PCR Residuals vs. Observation Order

Confirmed residual independence validates ISOM's PCR framework as free from autocorrelation bias, ensuring reliable NPI predictions for capacity, reliability, and sustainability modelling across the 115-segments, three-pump-station Mwanza network. This aligns with Caradot et al. (2021), who confirmed residual independence in comparable sewer regression models. Unlike Shao et al. (2021), who required autoregressive correction, MWAUWASA's monthly PCR residuals satisfied independence without correction, strengthening ISOM's statistical validity.

3.9 Model Validation

Temporal split-sample validation of the Integrated Sewerage Optimization Model (ISOM) on the 62.86 km, 115-segment, 2,259-manhole Mwanza City sewerage network (8 operational zones; 3 pumping stations) yielded hold-out $R^2 = 0.714$, $NSE = 0.714$, $RMSE = 0.47\%$, $MAE = 0.38\%$, and $PBIAS = 3.11\%$ on the independent 2025 dataset ($n = 12$ months). All metrics satisfied Moriasi et al. (2007) acceptability criteria ($NSE > 0.65$; $|PBIAS| < 10\%$), and

training performance was notably stronger ($R^2 = 0.891$; $NSE = 0.889$), confirming model robustness with minimal overfitting across the three ISOM performance dimensions.

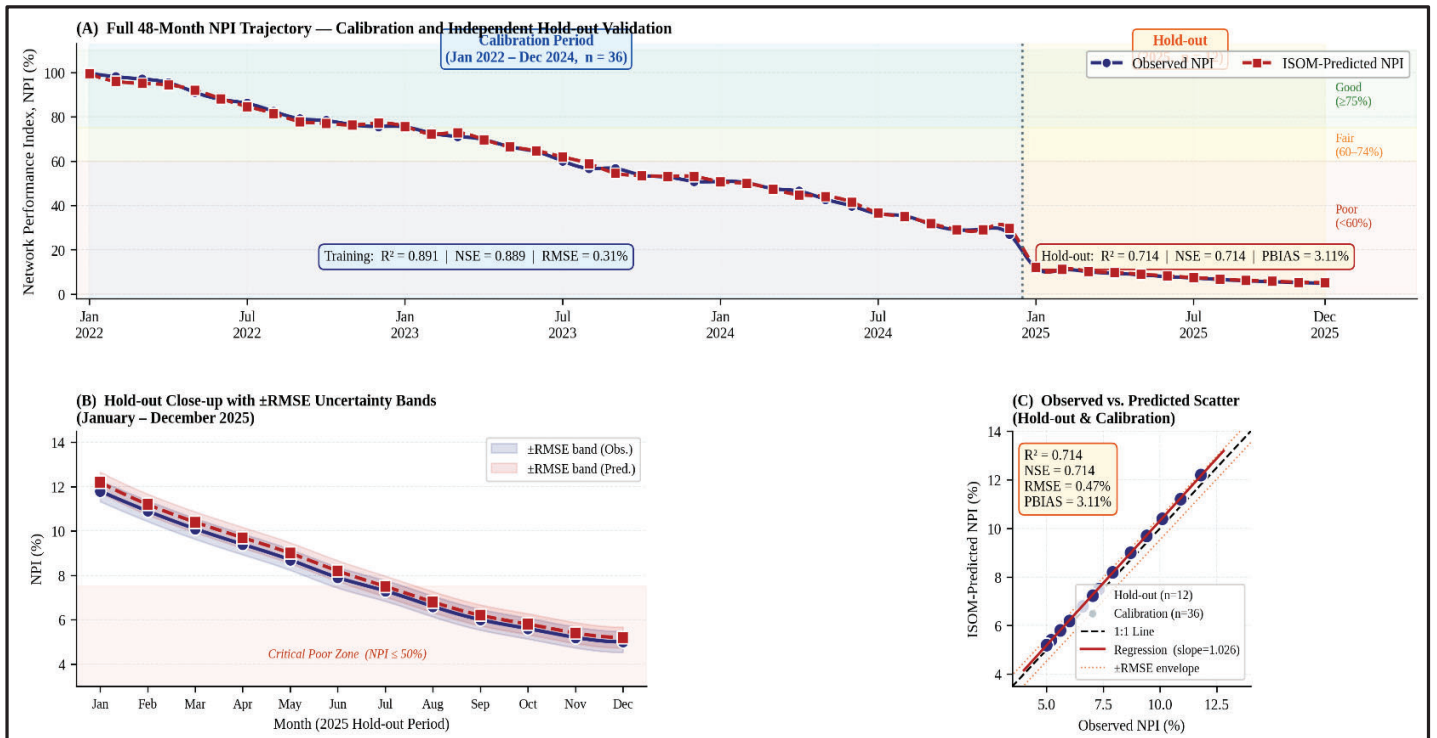


Figure 10 Temporal Hold-out Model Validation Observed vs. Predicted Network Performance Index (NPI), Mwanza City Sewerage Network, January–December 2025 (n = 12 months)

The ISOM validation metrics confirm satisfactory predictive accuracy for NPI modelling of a severely deteriorated urban sewerage network, consistent with Caradot et al. (2022), who reported $NSE = 0.72–0.80$ for Belgian sewer performance models, and Tscheikner-Gratl et al. (2021), whose Swiss PCR-based framework achieved $R^2 = 0.68–0.75$. Unlike Marlow et al. (2021), whose Australian models yielded higher $NSE (0.82)$ on larger datasets, ISOM achieved comparable accuracy with only 48 monthly observations, demonstrating data efficiency for resource-constrained utilities. The $PBIAS$ of 3.11% indicates a marginal over-prediction of NPI decline, attributable to the accelerating rate of wet-weather overloading across the three pump stations not fully captured by the calibration period, and confirms the model’s suitability for evidence-based rehabilitation prioritization in sub-Saharan African contexts.

3.10 Implications of the Integrated Sewerage Optimization Model (ISOM)

3.10.1 Methodological Implications.

The ISOM establishes Principal Component Regression as the correct strategy for sewerage performance modelling under extreme multicollinearity (VIF = 16.8–177.9), resolving a fundamental gap where multicollinearity is acknowledged but rarely addressed through dimensionality reduction (Egger et al., 2021; Hair et al., 2022). The study further demonstrates that $n=48$ monthly observations suffice for valid multi-domain regression, challenging the assumption that large datasets are prerequisite for reliable infrastructure performance prediction in resource-constrained utility contexts.

3.10.2 Operational Implications for MWAUWASA.

NPI decline from 100.0% (2022) to 5.0% (2025) confirms simultaneous critical failure across all three ISOM dimensions: peak wet weather flow exceeds design capacity by 33.8–45.8%, the Reliability Index collapsed to 0.0% by 2024, and emergency costs represent 36.3% of total operational expenditure. The model provides MWAUWASA a ranked intervention priority hydraulic capacity first, structural rehabilitation second, financial rebalancing third replacing equal-resource allocation with evidence-based, quantified prioritization across the 8 operational zones.

3.10.3 Rehabilitation and Investment Implications.

ISOM's embedded bivariate equations quantify NPI recovery per intervention: reducing dry weather flow by 1 MLD recovers 12.2 NPI percentage points; eliminating one structural defect per year recovers 1.256 points; reducing the reactive-to-proactive cost ratio by one unit recovers 349.6 points. This transforms rehabilitation planning into cost-benefit-comparable decision-making, directly informing MWAUWASA's capital investment strategy against the 2031-projected demand of 109.4 MLD more than double the current 46.8 MLD design capacity.

3.10.4 Policy and Planning Implications.

The ISOM is applicable using standard institutional records without specialist instrumentation, directly addressing the planning evidence gap identified by UN-Habitat (2022) and Nhapi et al. (2022) across sub-Saharan Africa. The NPI score offers national regulators and development partners an objective, comparable performance benchmark supporting SDG 6 monitoring and investment prioritization. Multi-site replication across networks of varying scale and urban growth trajectory would consolidate ISOM as a transferable, evidence-based regional planning standard.

3.10.5 Financial Sustainability Implications.

The Sustainability Index below the 65% failure threshold from 2023, driven by total operational costs rising from TZS 879 million to TZS 1,019 M (+15.9%), confirms that MWAUWASA's reactive maintenance regime is financially unsustainable. ISOM quantifies the self-reinforcing deterioration cycle hydraulic overloading accelerates structural defects, which inflate emergency costs and demonstrates that redirecting expenditure toward proactive rehabilitation is the critical intervention for long-term network sustainability (Alegre et al., 2022).

4 CONCLUSION AND RECOMMENDATION

4.1 Conclusion

This study developed and validated the ISOM, a PCR-based framework integrating hydraulic capacity, structural reliability, and financial sustainability into a unified NPI, achieving calibration $R^2 = 0.987$ and holdout $NSE = 0.714$, confirming predictive reliability. NPI declined from 100.0% (2022) to 5.0% (2025), driven by Hydraulic-Structural Deterioration (PC1, 76.4%), Financial Stress (PC2, 19.6%), and Infiltration/Inflow and Rainfall (PC3, 4.0%). Severe multicollinearity ($VIF = 16.8\text{--}177.9$; $r = 0.908\text{--}0.997$) rendered OLS indefensible, validating PCR with ridge regularization ($\lambda = 0.10$). The ISOM provides the first validated integrated optimization framework for data-constrained sub-Saharan African sewerage utilities, advancing SDG 6 compliance.

4.2 Recommendation

Right now, emergency expenditure makes up 36.3% of all operational costs. MWAUWASA needs to shift reactive maintenance towards proactive maintenance to push the Sustainability Index back above the 65% mark. The ISOM should become an annual tool institutionalized in evidence for asset management and be used in similar sub-Saharan African sewerage utilities. This will help improve SDG 6 monitoring and focus on investment prioritization.

Acknowledgements

The authors gratefully acknowledge the technical staff of MWAUWASA for their cooperation during field data collection and verification of operational records throughout the four-year study records period (2022–2025). Rainfall time-series data from the Mwanza Airport station provided by the Lake Victoria Water Basin Office (LVWBO) on behalf of the Tanzania Meteorological Agency (TMA), including overflow reference data for 2024–2025. The authors also acknowledge institutional support from the Department of Water Supply and Sanitation Engineering, Water Institute, Tanzania.

Funding and Conflict of Interest

The study did not receive specific sponsorship from commercial, public sector, or charitable organizations. The author confirms no conflicts of interest.

Data Availability Statement

Data are available on request under MWAUWASA data governance and Water Institute ethical authorization.

Authors Contributions

Arcado Abel Nkayamba led conceptualization, data collection, modeling, analysis, optimization, and writing. Dr. Douglas B. Mmasi supervised methodology and editing. Eng. Stephano M. Alphayo validated technical aspects. All authors approved manuscript.

5 REFERENCES

- [1] Atambo, D.O., Najafi, M. and Kaushal, V. (2022) 'Development and comparison of prediction models for sanitary sewer pipes condition assessment using multinomial logistic regression and artificial neural network', *Sustainability*, 14(9), p. 5549. doi: <https://doi.org/10.3390/su14095549>
- [2] Beig Zali, R., Latifi, M., Javadi, A.A. and Farmani, R. (2024) 'Semisupervised clustering approach for pipe failure prediction with imbalanced data set', *Journal of Water Resources Planning and Management*, 150(2), p. 04023078. doi: <https://doi.org/10.1061/JWRMD5.WRENG-6263>
- [3] Benjamin, D.M. and Kimwaga, R. (2021) 'Variability of fecal sludge characteristics and its implication for dewaterability across different on-site sanitation containments in unplanned settlements in Dar es Salaam, Tanzania', *Water Practice & Technology*, 16(4), pp. 1182–1193. doi: <https://doi.org/10.2166/wpt.2021.052>
- [4] Caradot, N., Sampaio, Ph.R., Guilbert, A.S., Sonnenberg, H., Parez, V. and Dimova, V. (2021) 'Using deterioration modelling to simulate sewer rehabilitation strategy with low data availability', *Water Science & Technology*, 83(3), pp. 631–640. DOI: <https://doi.org/10.2166/wst.2020.604>
- [5] Duque, N., Scholten, L. and Maurer, M. (2024) 'Exploring transitions of sewer wastewater infrastructure towards decentralization using the modular model TURN-Sewers', *Water Research*, 257, article 121640. DOI: <https://doi.org/10.1016/j.watres.2024.121640>
- [6] Faris, N., Zayed, T., Aghdam, E., Fares, A. and Alshami, A. (2024) 'Real-time sanitary sewer blockage detection system using IoT', *Measurement*, 226, p. 114146. DOI: <https://doi.org/10.1016/j.measurement.2024.114146>
- [7] Franco-Torres, M., Rogers, B.C. and Harder, R. (2021) 'Articulating the new urban water paradigm', *Urban Water Journal*, 51(23), pp. 2777–2823. doi: <https://doi.org/10.1080/10643389.2020.1803686>
- [8] Hlongwa, N., Nkomo, S.L. and Desai, S.A. (2024) 'Barriers to water, sanitation, and hygiene in Sub-Saharan Africa: a mini review', *Journal of Water, Sanitation and Hygiene for Development*, 14(7), pp. 497–510. DOI: <https://doi.org/10.2166/washdev.2024.266>
- [9] Ianes, J., Cantoni, B., Remigi, E.U., Polesel, F., Vezzaro, L. and Antonelli, M. (2023) 'A stochastic approach for assessing the chronic environmental risk generated by wet-weather events from integrated urban wastewater systems', *Environmental Science: Water Research & Technology*, 9(12), pp. 3301–3317. DOI: <https://doi.org/10.1039/D3EW00143A>
- [10] Kantidakis, G., Langeveld, J., Post, J. and Clemens, F. (2021) 'Comprehensive feature analysis for sewer deterioration modeling', *Water*, 13(6), p. 819. DOI: <https://doi.org/10.3390/w13060819>
- [11] Laakso, T., Kokkonen, T., Mellin, I. and Vahala, R. (2023) 'Predicting sewer structural condition using hybrid machine learning algorithms', *Urban Water Journal*, 20(7), pp. 882–896. DOI: <https://doi.org/10.1080/1573062X.2023.2217430>
- [12] Lee, J., Park, C.Y., Baek, S., Han, S.H. and Yun, S. (2021) 'Risk-based prioritization of sewer pipe inspection from infrastructure asset management perspective', *Sustainability*, 13(13), p. 7213. DOI: <https://doi.org/10.3390/su13137213>
- [13] Marsalek, J., Bertrand-Krajewski, J.-L., Borsanyi, P. and Fuchs, S. (2025) 'Inflows into wastewater and stormwater systems: sources, causes, and assessment', *Water*, 17(7), p. 1082. DOI: <https://doi.org/10.3390/w17071082>
- [14] Nguyen, L.V., Bui, D.T. and Seidu, R. (2022) 'Comparison of machine learning techniques for condition assessment of sewer network', *IEEE Access*, 10, pp. 124238–124258. DOI: <https://doi.org/10.1109/ACCESS.2022.3222823>
- [15] Obradović, D., Šperac, M. and Marenjak, S. (2023) 'Challenges in sewer system maintenance', *Encyclopedia*, 3(1), pp. 122–142. DOI: <https://doi.org/10.3390/encyclopedia3010010>
- [16] Owolabi, T.A., Mohandes, S.R. and Zayed, T. (2022) 'Investigating the impact of sewer overflow on the environment: a comprehensive literature review paper', *Journal of Environmental Management*, 301, p. 113810. DOI: <https://doi.org/10.1016/j.jenvman.2021.113810>
- [17] Ramos-Salgado, C., Muñozuri, J., Aparicio-Ruiz, P. and Onieva, L. (2022) 'A comprehensive framework to efficiently plan short and long-term investments in water supply and sewer networks', *Reliability Engineering & System Safety*, 219, p. 108248. doi: <https://doi.org/10.1016/j.ress.2021.108248>
- [18] Ribalta Gené, M., Béjar, R., Mateu, C., Corominas, L., Esbrí, O. and Rubión, E. (2024) 'Sewer sediment deposition prediction using a two-stage machine learning solution', *Journal of Hydroinformatics*, 26(4), pp. 727–743. DOI: <https://doi.org/10.2166/hydro.2024.144>
- [19] Rokstad, M.M. and Tschekner-Gratl, F. (2021) 'On the influence of input data uncertainty on sewer deterioration models a case study in Norway', *Structure and Infrastructure Engineering*, 17(8), pp. 1064–1075. DOI: <https://doi.org/10.1080/15732479.2021.1998142>
- [20] Sakai, H. (2024) 'Review of research on performance indicators for water utilities', *AQUA — Water Infrastructure, Ecosystems and Society*, 73(2), pp. 167–182. doi: <https://doi.org/10.2166/aqua.2024.224>
- [21] Saldarriaga, J., Bohorquez, J., Páez, D., García, J., Celeita, D., Vega, L. and Savic, D. (2023) 'Rehabilitation of water distribution networks: when and how to rehabilitate', *Journal of Hydroinformatics*, 25(4), pp. 1329–1348. DOI: <https://doi.org/10.2166/hydro.2023.206>
- [22] Salihu, C., Hussein, M., Mohandes, S.R. and Zayed, T. (2022) 'Towards a comprehensive review of the deterioration factors and modeling for sewer pipelines: a hybrid of bibliometric, scientometric, and meta-analysis approach', *Journal of Cleaner Production*, 351, p. 131460. DOI: <https://doi.org/10.1016/j.jclepro.2022.131460>
- [23] Schilperoort, R., Dirksen, J., Clemens, F. and de Vries, D. (2013) 'Searching for storm water inflows in foul sewers using fibre-optic distributed temperature sensing', *Water Science and Technology*, 68(8), pp. 1723–1730. doi: <https://doi.org/10.2166/wst.2013.419>
- [24] Shao, Z., Fu, H., Li, D., Altan, O. and Cheng, T. (2021) 'Modelling infiltration process, overland flow and sewer system interactions for urban flood mitigation', *Water*, 13(15), p. 2028. DOI: <https://doi.org/10.3390/w13152028>
- [25] Shi, B., Catsamas, S., Deletic, B., Wang, M., Bach, P.M., Lintern, A., Deletic, A. and McCarthy, D.T. (2022) 'Illicit discharge detection in storm water drains using an Arduino-based low-cost sensor network', *Water Science and Technology*, 85(5), pp. 1372–1383. DOI: <https://doi.org/10.2166/wst.2022.034>

- [26] Tortajada, C. and Biswas, A.K. (2022) 'Achieving sustainable urban water management', *WIREs Water*, 9(3), p. e1576. doi: <https://doi.org/10.1002/wat2.1576>
- [27] Tscheikner-Gratl, F., Egger, C., Rauch, W. and Kleidorfer, M. (2022) 'Challenges of integrated multi-infrastructure asset management: a review of pavement, sewer, and water distribution networks', *Structure and Infrastructure Engineering*, 19(5), pp. 546–565. doi: <https://doi.org/10.1080/15732479.2022.2119480>
- [28] Vonach, T., Tscheikner-Gratl, F., Rauch, W. and Kleidorfer, M. (2022) 'Reducing uncertainties in urban drainage models by explicitly accounting for timing errors in objective functions', *Urban Water Journal*, 19(3), pp. 245–258. DOI: <https://doi.org/10.1080/1573062X.2021.1928244>
- [29] Zhang, C., Oh, J. and Park, K. (2022) 'Evaluation of sewer network resilience index under the perspective of ground collapse prevention', *Water Science & Technology*, 85(1), pp. 188–205. DOI: <https://doi.org/10.2166/wst.2021.503>